# I: TITLE PAGE

# Impact of Acute Endurance Exercise on Alternative Splicing in Skeletal Muscle.

Alexander Ahn, MS[1]

ORCID: 0009-0009-7865-2061

Ann Arbor, Michigan, USA

November 21, 2024

Co-authors:

i. Jeongjin J. Kim, PhD[1,2] (ORCID: 0000-0002-6959-8544; now at Frederick, Maryland, USA)
ii. Aaron L. Slusher, PhD[1,3] (ORCID: 0000-0003-2082-4827; now at New Haven, Connecticut, USA)
iii. Jeffrey Y. Ying[1] (no ORCID; Ann Arbor, Michigan, USA)
iv. Eric Y. Zhang[1] (ORCID: 0009-0000-7975-0303; Ann Arbor, Michigan, USA)

Corresponding author: Andrew T. Ludlow, PhD[1]

- ORCID: 0000-0003-0423-4800; Ann Arbor, Michigan, USA
- 830 North University Avenue, Ann Arbor, Michigan 48109-1048, USA
- atludlow@umich.edu
- +1 (734) 763-4720

Affiliation:

1. School of Kinesiology, University of Michigan, Ann Arbor, Michigan, USA
2. National Cancer Institute, National Institutes of Health, Frederick, Maryland, USA
3. School of Medicine, Yale University, New Haven, Connecticut, USA

# II: ABSTRACT

**Purpose:** Alternative RNA splicing (AS) is a highly conserved post-transcriptional mechanism, generating mRNA variants to diversify the proteome. Acute endurance exercise appears to transiently perturb AS in skeletal muscle, but transcriptome-wide responses are not well-defined. We aimed to better understand differential AS (DAS) in skeletal muscle by comparing short-read RNA sequencing (SRS) and long-read RNA sequencing (LRS) data.

**Methods:** Publicly accessible SRS of clinical exercise studies were extracted from the Gene Expression Omnibus. Oxford Nanopore LRS was performed on mouse gastrocnemius before and following treadmill exercise. Differential gene expression (DGE), DAS, and isoform switching were analyzed. Western blots were performed to validate expression changes of candidate genes.

**Results:** Both SRS and LRS illustrated significant DGE in skeletal muscle post-exercise, whereby 57 and 15 RNA-binding proteins (RBPs) were up-/down-regulated, respectively. rMATS analysis of SRS data revealed that exon-skipping and intron-retaining splicing events were the most common. Swan analysis of LRS data revealed 38 RBPs with significant isoform switching: one of these RBPs, *Hnrnpa3*, underwent a significant intron-retained to protein-coding switch. HnRNP-A3 protein levels validated nearly two-fold increases at 1 hour ($p$=.0043) and 24 hours ($p$=.0103) post-exercise.

**Conclusions:** This study illustrates that acute endurance exercise can elicit changes in AS-related responses and RBP expression in skeletal muscle. SRS is certainly a powerful tool for analyzing DGE but lacks AS detection. As such, “hidden” genes with no transcriptional changes but significant DAS and protein expression changes pose a major gap in knowledge. Our work highlights how LRS can uncover previously unknown transcript diversity and mechanisms influencing endurance exercise adaptations and responses.

**Keywords**

Endurance exercise, alternative RNA splicing, RNA-binding proteins, splicing factors, skeletal muscle.

**Abbreviations**

A3SS, alternative 3' splice site;

A5SS, alternative 5' splice site;

AS, alternative (RNA) splicing;

ATSS, alternative transcription start site;

ATTS, alternative transcription termination site;

DAS, differential alternative splicing;

DGE, differential gene expression;

hsAA, *homo sapiens* aged active;

hsAS, *homo sapiens* aged sedentary;

hsYS, *homo sapiens* young sedentary;

lncRNA, long non-coding RNA;

LRS, long-read RNA sequencing;

mmYS, *mus musculus* young sedentary;

MXE, mutually exclusive exons;

pcRNA, protein-coding RNA;

RBP, RNA-binding protein;

RI, retained intron;

SE, skipped exon;

SRS, short-read RNA sequencing.

# III: BODY

## 1 INTRODUCTION

The positive impact of exercise on one's health is undeniable. With skeletal muscle accounting for approximately 40% of body mass in adults, it is the most directly affected tissue from both the beneficial effects of physical activity as well as the deleterious effects of sedentarism. However, a large portion of the population fails to meet the minimum amount of exercise to reduce health risks. The US Centers for Disease Control and Prevention reported overall prevalence of physical inactivity was 25.3% in 2020,[1] while causing 9% of premature death globally.[2] Why people fail to meet the minimum amount of exercise are varied but some are simply unable to even if desired: for example, muscle dystrophy, motoneuron-related sclerosis diseases, and obesity-induced osteoarthritis. To fully harness the health-promoting power of endurance exercise, we must continue to uncover the fundamental mechanisms of molecular responses and adaptations elicited by the exercise stimulus.

Endurance exercise promotes disease-free longevity via the enhancement of skeletal muscle oxidative capacity among other important responses and adaptations.[3] Exercise is a potent cellular stressor (eg, mechanical, metabolic, oxidative stress, etc) that triggers a series of responses and adaptations.[4–7] Part of the adaptive process in skeletal muscle is changes in gene expression regulation that, in part, regulates the protein landscape and alters structural and functional outcomes. To date, reports have focused on changes in transcript levels, differential gene expression (DGE).[8,9] For example, endurance exercise training increases mitochondrial density, muscle-specific angiogenesis, and improves calcium handling in slow-twitch skeletal myofibers by altering the expression of the genes encoding peroxisome proliferator-activated receptor gamma coactivator 1 alpha (PGC-1α, *PPARGC1A*),[10] vascular endothelial growth factor

(*VEGF*),[11] and troponin T (ssTnT, *TNNT1*),[12] respectively. While *PPARGC1A*, *VEGF*, and *TNNT1* are all differentially expressed, there is also evidence that exercise impacts the expression of different transcript variants of each of these genes,[12–15] indicating that alternative RNA splicing (AS) is impacted by exercise.[16,17] To date, however, only one group has investigated mRNA isoform expression using SRS following exercise training in human skeletal muscle and observed global training induced changes in mRNA isoform expression.[16]

RNA splicing and AS are RNA processing steps that offer additional regulatory layers in gene expression. RNA splicing is mediated by a dynamic RNA-protein complex, the spliceosome, that assembles on primary transcripts (ie, precursor messenger RNA, pre-mRNA) to remove introns and splice exons together to form the final protein-coding transcript (ie, mature messenger RNA, mRNA).[18] In conjunction with the spliceosome, RNA-binding proteins (RBPs) provide tissue-/context-specific regulation of splicing.[19] While most exons of a pre-mRNA undergo constitutive splicing to form full-length variants, many undergo AS: the choice of including or excluding certain exons and/or introns in the mRNA.[20,21] AS is a highly conserved co-/post-transcriptional mechanism that functions to generate multiple RNA transcript variants: these transcript variants may be intended for either translation to respective protein isoforms,[22,23] non-coding RNAs,[24,25] or degradation via RNA decay mechanisms.[26,27] Therefore, a single gene can form several protein isoforms depending on the demands of the cells in a tissue.[22] For instance, a significant change in AS can orchestrate a switch in the expression of certain protein isoforms. These differential use of isoforms between conditions is often referred as isoform switching,[13,14] which facilitate a functional change in cellular responses to stimuli. The significance of AS is evident as nearly all mammalian genes undergo AS and generate two or more protein isoforms, which vastly expands the protein-coding capacity of the genome and

greatly impacts the function of cells in a tissue and cells responses to homeostatic perturbations.[22]

However, transcriptome-wide impact of endurance exercise on AS and isoform generation is currently unknown. Previously, Tonevitsky et al[28] observed that acute aerobic exercise with maximal intensity in trained skiers resulted in an increased gene expression from a set of RBPs (*DDX17*, *DDX46*, *HNRNPR*, *PRPF4B*, and *SRPK2*) that regulate the formation of the precatalytic spliceosome. Similarly, our laboratory also observed that exercise resulted in reduced protein expression of splicing factor 3B subunit 4 (SF3B4) from young sedentary mouse gastrocnemius in response to acute treadmill running.[29] These findings indicate that a single bout of endurance exercise is sufficient to potentially instigate differential AS (DAS) and differential isoform usage of many other genes through differential expression and regulation of RBPs. Therefore, we set out to globally profile AS events (mRNA variants and exon-level events) in skeletal muscle from a single bout of submaximal endurance exercise.

# 2 MATERIALS AND METHODS

## 2.1 Short-read RNA sequencing

The human SRS data had formerly been published by two different studies: Pattamapraponont et al[30] and Rubenstein et al.[31] The raw FASTQ files were downloaded from publicly accessible NCBI Gene Expression Omnibus database (RRID: SCR_005012) (accession numbers GSE87749 and GSE151066, respectively). Briefly, Pattamapraponont et al consisted of 10 young (19-25 years) and healthy (BMI of 23.1 ± 2.8) Danish male participants with a sedentary lifestyle (hsYS), and performed a single bout of intense (80% $V\square O_2$max) cycling (cycle ergometer) for 15 minutes; muscle biopsies of the vastus lateralis were obtained pre- (hsYS-pre) and 4 hours post-exercise (hsYS-4pe).[30] Rubenstein et al studied two cohorts of older individuals (65-90 years): 10 (8 males, 2 females) an active/endurance trained group (hsAA) with a BMI of 24.2 ± 4.2; nine (7 males, 2 females)and a sedentary (hsAS) group with a BMI of 28.7 ± 3.3. The participants performed a single bout of endurance exercise (cycling at 60-70% of heart rate reserve) for 40 minutes. Muscle biopsies of the vastus lateralis were obtained pre- (hsAA-pre & hsAS-pre) and 3 hours post-exercise (hsAA-3pe & hsAS-3pe).[31] To maintain consistency for the initial processing and statistical analyses of the SRS data, only single-end FASTQ files were used from the Pattamaprapanont et al study; similarly, only males at pre- and 3 hours post-exercise time points with paired-end FASTQ files were used from the Rubenstein et al to maintain comparability between the two data sets (Figure 1A).

## 2.2 Animals

All animal experiments were approved by the University of Michigan Institutional Animal Care and Use Committee (IACUC) and conducted as per the institutional guidelines. C57BL/6-Tg(TERT)C10Hode/J (approximately 8 weeks old) were purchased from The Jackson

Laboratory (Bar Harbor, Maine, USA). The mice were housed at 25°C on a 12:12-hour light-dark cycle, fed *ad libitum* laboratory mouse chow (Prolab® RMH 3000, 5P00, LabDiet by Purina, Nestlé, Vevey, Switzerland), and given free access to water. The description of the running protocol was previously published.[29] Animals were randomly assigned to each pre-/post-exercise time points. All animals were included without exclusion nor attrition. Investigators were not blinded to the groupings. Sample size and power analysis were determined based on our previous study.[29] Briefly, 20 mice underwent acute treadmill running at 60% of maximal speed, approximately 75% of mouse $VO_2$max according to Fernando et al,[32] for 30 minutes (Figure 1B,S1M). Euthanasia practices were followed as suggested by the American Veterinarian Medical Association guidelines (2020 edition). Gastrocnemius muscles were collected at pre- (mmYS-pre; 3 males, 2 females), immediately post-exercise (mmYS-ipe; 3 males, 2 females), 1 hour post-exercise (mmYS-1pe; 2 males, 3 females), and 24 hours post-exercise (mmYS-24pe; 3 males, 2 females). Gastrocnemius muscles were flash frozen in liquid nitrogen and stored at –80°C for subsequent tissue processing and RNA isolation.

## 2.3 Tissue processing, RNA isolation, and poly(A)-mRNA isolation

The gastrocnemius tissues were first powdered with a mortar and pestle in liquid nitrogen, then either processed immediately or stored at –80°C, as described in Slusher et al.[29] Total RNA from powdered tissues were isolated using the RNeasy Plus Universal Mini Kit (Qiagen, Cat# 73404) according to manufacturer instructions, and stored at -80°C. Isolated RNA was quantified using the NanoDrop™ 2000 spectrophotometer and assessed using the Qubit™ RNA IQ Assay Kits (Invitrogen, Cat# Q33221) with the Qubit 4 Fluorometer. Subsequently, 1.2 µg of total RNA was used to isolate poly(A)-containing RNA with the NEBNext® Poly(A) mRNA Magnetic Isolation Module (New England BioLabs, Cat# E7490S) accordingly. Poly(A)-mRNA isolates

were then quantified with Agilent Bioanalyzer (RRID: SCR_018043) and/or TapeStation, NanoDrop™ 2000 spectrophotometry, and Qubit Fluorometry.

## 2.4 Long-read RNA sequencing

1 ng of poly(A)-mRNA isolates were used to synthesize barcoded PCR-cDNA libraries (Oxford Nanopore Technologies®, ONT; Cat# SQK-PCB109) according to the manufacturer instructions. Subsequently, the prepared PCR-cDNA libraries were quantified, multiplexed at equal molar concentrations, loaded onto a MinION™ R9.4.1 Flow Cell (ONT, Cat# FLO-MIN106) and sequenced (LRS) for 72 hours (protocol on the MinION™ Mk1C sequencer (ONT, Cat# MIN-101C) under MinKNOW v22.03.4 (ONT, RRID: SCR_023196); Figure 1B). During the sequencing period, the flow cell was "washed" with the Flow Cell Wash Kit (ONT, Cat# EXP-WSH004) and reloaded with fresh multiplexed libraries as needed.

## 2.5 Data preprocessing

For the SRS retrieved data, the quality of the raw FASTQ files were checked and trimmed to the minimum read length of 25 bases. Subsequently, RSEM-STAR[33,34] was used to align and quantify the trimmed reads based on the human GENCODE release 42 (GRCh38.p13). Matrices of "counts" (estimation of expected read counts), "abundance" (TPM-normalized counts), and "length" (effective transcript lengths) were generated for statistical analyses (hsYS: Figure S1A,E,I; hsAS: Figure S1B,F,J; and hsAS: Figure S1C,G,K).

For the LRS generated data, raw FASTQ (converted from FAST5) files, which passed the MinKNOW quality check with minimum *q*-score threshold of 8, were used for read alignment. minimap2 v2.14[35] (RRID: SCR_018550) and SAMtools v1.13[36] (RRID: SCR_002105) was used to align the passed FASTQ files into SAM format; the mouse GENCODE release M29 (GRCm39) genome sequence assembly was used for the alignment step. The aligned SAM files

were sorted and "cleaned" (TranscriptClean[37]). TALON[38] was used to quantify reads and generate an abundance matrix (coverage = 0.75, identity = 0.8) in GTF format to be used for statistical analyses (Figure S1D,H,L and Figure S4D,E).

## 2.6 Differential gene expression and differential alternative splicing analyses

For the SRS-retrieved data, TXImport[39] was used to import the multidimensional RSEM-STAR quantification matrix arrays at the gene-level to the R environment. Subsequently, DESeq2[40] was used to perform gene-level differential expression (differential gene expression, DGE) analyses with $\log_2$ fold changes ($\log_2$FC) and respective statistics (*p*-values adjusted with default Benjamini-Hochberg method, BH; *p*-adj) on the quantification matrix arrays, and enriched for significantly up-/down-regulated genes (Figure 2A–G). IsoformSwitchAnalyzeR[41] was initially used (Figure S2) to identify genes with isoform-switching events with absolute difference in isoform fraction (dIF) > 10% and *p*-adj < .05 (adjusted with BH). Splicing type resulting in the isoform switches were annotated as skipped exon (SE), alternative 5' splice site (A5SS), alternative 3' splice site (A3SS), mutually exclusive exons (MXE), multiple exon-skipping (MES), retained introns (RI), alternative transcription start site (ATSS), and alternative transcription termination site (ATTS). Additionally, rMATS-turbo v4.1.2[42,43] was used to directly analyze exon-level splicing events with difference in percent spliced in ($\Delta\Psi$ or DPSI) and respective statistics on the trimmed FASTQ files, and enriched for genes with significant splicing events annotated as SE, A5SS, A3SS, MXE, and RI. The transcript-level rMATS data frames were filtered based on the absolute $\Delta\Psi$ > 10% and *p*-adj < .05 (adjusted with BH) for the significant splicing overlap analyses and for visualizing the proportions of splicing profile.

For the LRS-generated data, Swan v2.0[44] was used to generate data frames with $\log_2$FC and respective significance statistics at the gene- and transcript-levels. Based on known genes

that were detected in at least half of the samples, the counts matrix was generated for the downstream differential analyses. The corresponding DGE (gene-level) $\log_2$FC and respective statistics (adjusted with BH) from Swan were used for data visualizations (Figure 2H–J). Similarly, differential isoform expression analyses generated absolute difference in percent isoform use (ΔΠ or DPI) to determine isoform-switching data, whereby respective statistics from Swan were filtered based on ΔΠ > 10% and *p*-adj < .05 (adjusted with BH).

Functional enrichment analysis was performed on significantly up- and down-regulated genes from the DGE analyses ($|\log_2 FC| > 1.5$ and *p*-adj < .05 for SRS; $|\log_2 FC| > 1$ and raw *p* < .05 for LRS) using either Database for Annotation, Visualization, and Integrated Discovery (DAVID)[45] or PANTHER[46] (for Figure S4A–C only) to generate top 10 gene ontology (GO) terms. With the splicing and DIE data sets from both SRS and LRS data, multiple multivariate overlap analyses across varying conditions and data sets were performed to identify any common genes with potential biologically significant splicing events. Only overlapping genes with *p*-adj < .05 from bivariate hypergeometric tests were considered significant. All code scripts used for bioinformatical data analyses are available in the Deep Blue data repository (DOI will be provided upon publication) or upon request.

## 2.7 Protein lysate preparation, antibody validation, and western blot analyses

To examine protein expression level of a candidate RBP, heterogeneous nuclear ribonucleoprotein A3 (hnRNP-A3), HEK 293 fetal kidney cells (ATCC, Cat# CLR-1573, RRID: CVCL_0045) were used as positive controls to verify cross-species specificity of the hnRNP-A3 antibody for the correct molecular weight at 42 kDa. Additionally, C2C12 murine myoblasts (ATCC, Cat# CRL-1772, RRID: CVCL_0188) were transfected with 30 nM of either scrambled (siCTL) or mouse *Hnrnpa3*-targeting (exon 10) siRNAs (ThermoFisher Scientific, Cat# 4390771)

in Lipofectamine™ RNAiMAX transfection reagent (Invitrogen, Cat# 13778075) for 24 and 48 hours to knock-down hnRNP-A3 and thus validate the protein specificity of hnRNP-A3 antibody. All cell lines used were authenticated by the manufacturer (ATCC) and visually verified in-house. The cell pellets were resuspended in an SDS-based lysis buffer, sonicated, and centrifuged to extract the total protein lysate. Total protein lysates were prepared from gastrocnemius, as described in Slusher et al,[29] were used to quantify protein expression level of hnRNP-A3 in the skeletal muscle tissues. The protein concentrations were quantified using the Pierce 660 nm Protein Assay Kit (ThermoFisher Scientific, Cat# 1861426). These protein lysates from cell lines and the animal-derived tissues were then prepared using 2X Laemmli loading buffer (Bio-Rad, Cat#1610737) and boiled for 10 minutes at 95°C.

All protein lysates from cells and tissues were resolved by SDS-polyacrylamide gel electrophoresis, transferred to polyvinylidene fluoride membranes. To verify cross-species specificity of the hnRNP-A3 antibody, protein lysates of wild-type HEK 293 was used (Figure S5A). Loading control was normalized with GAPDH (Cell Signaling Technology, Cat# 2118, RRID: AB_561053; 1:1000 dilution in 5% bovine serum albumin with 1X PBST). To validate protein specificity of the hnRNP-A3 antibody, protein lysates of C2C12 myoblasts treated with either siCTL or *Hnrnpa3* siRNA were used (Figure S5B,C). Loading control was normalized with total protein quantification of bands at 40-45 kDa using Pierce™ Reversible Protein Stain Kit (ThermoFisher Scientific, Cat# 24585). HnRNP-A3 from these cell lysates was detected with a rabbit polyclonal antibody (Abcam, Cat# ab78300, RRID: AB_2041662; 1:1000 dilution factor in 5% bovine serum albumin with 1X PBST and 0.02% sodium azide). Loading control of protein lysates from the skeletal muscle tissue was normalized with total protein quantification of bands at 40-45 kDa using Ponceau S stain (Sigma-Aldrich, Cat# P3504) and detected for

hnRNP-A3 with the validated polyclonal antibody. All blots were imaged with Bio-Rad ChemiDoc XRS+ Molecular Imager (RRID: SCR_019690) and quantified with Bio-Rad Image Lab software. Values from either the reversible Pierce-/Ponceau S-stained blots (tissue-based lysates) or the loading control blots (cell-based lysates) were averaged and used to normalize the target protein quantification. All images that were used to quantify hnRNP-A3 expression levels are included in Figure S5D.

## 2.8 Statistical analysis

Unless otherwise noted, unpaired Student's *t* test was used for two group comparisons using a statistical package on GraphPad Prism 10 (RRID: SCR_002798). One-way ANOVAs were used to determine significance for multiple group comparisons of the western blot data, whereby the groups (time points) had 1 level each. Subsequently, *post hoc* adjustments were conducted with Tukey's HSD using GraphPad Prism 10. Statistical significance was defined as a $p < .05$.

# 3 RESULTS

## 3.1 RNA-Seq identified differential gene expression in acutely exercised skeletal muscle with and without training

Differential gene expression (DGE) of vastus lateralis in hsYS-pre and hsYS-4pe was analyzed with DESeq2 (Figure 2A): out of 13727 total detected genes, 19 were significantly up-regulated ($\log_2$FC > 1.5, *p*-adj < .05) including *PPARGC1A* (i.e., PGC-1α), *NR4A3*, and *HSPA1A/B* (i.e., HSP70), while 10 were significantly down-regulated ($\log_2$FC < −1.5, *p*-adj < .05). These significantly up-regulated genes revealed top 10 gene ontology (GO) terms with DAVID functional enrichment analysis (Figure 2B), including protein binding (GO:0005515, 15 genes, $p = 0.0596$), extracellular region (GO:0005576, 8 genes, $p = 7.6359e^{-4}$), and nucleoplasm (GO:0005654, 7 genes, $p = 0.0773$). Three GO terms were revealed from the significantly down-regulated genes (Figure 2C), including cell differentiation (GO:0030154, 3 genes, $p = 0.0419$), positive regulation of JNK cascade (GO:0046330, 2 genes, $p = 0.0449$), and response to peptide hormone (GO:0043434, 2 genes, $p = 0.0247$).

DGE of vastus lateralis in hsAS-pre and hsAS-3pe was analyzed (Figure 2D): out of 14082 total detected genes, 201 were significantly up-regulated ($\log_2$FC > 1.5, *p*-adj < .05) including *PPARGC1A*, *NR4A3*, and *HSPA1B*, while 9 were significantly down-regulated ($\log_2$FC < −1.5, *p*-adj < .05). These significantly up-regulated genes revealed top 10 GO terms with DAVID functional enrichment analysis (Figure 2E), including protein binding (GO:0005515, 141 genes, $p = 1.1661e^{-4}$), nucleus (GO:0005634, 72 genes, $p = 0.0020$), and plasma membrane (GO:0005886, 64 genes, $p = 0.0050$). Zero terms were significantly enriched from the down-regulated genes.

DGE of vastus lateralis in hsAA-pre and hsAA-3pe was analyzed (Figure 2F): out of 14315 total detected genes, 112 were significantly up-regulated ($\log_2$FC > 1.5, *p*-adj < .05) including *PPARGC1A*, *NR4A3*, *NR4A1*, and *HSPA1B*, while 4 were significantly down-regulated ($\log_2$FC < −1.5, *p*-adj < .05). These significantly up-regulated genes revealed top 10 GO terms with DAVID functional enrichment analysis (Figure 2G), including protein binding (GO:0005515, 79 genes, $p = 0.0058$), nucleus (GO:0005634, 47 genes, $p = 3.5854e^{-4}$), and plasma membrane (GO:0005886, 34 genes, $p = 0.0856$). Zero terms were revealed from the down-regulated genes.

DGE of gastrocnemius in mmYS-pre and mmYS-1pe was analyzed (Figure 2H): out of 2738 total detected genes, 6 were significantly up-regulated ($\log_2$FC > 1.0, raw $p < .05$), while 20 were significantly down-regulated ($\log_2$FC < −1.0, raw $p < .05$). These significantly up-regulated genes revealed 4 GO terms with DAVID functional enrichment analysis (Figure 2I). Six GO terms were revealed from the significantly down-regulated genes (Figure 2J).

## 3.2 Differentially expressed RNA-binding proteins in acutely exercised skeletal muscle with and without training

Using a list of 1135 RBP genes generated in house, significant up- ($\log_2$FC > 0.5) and down-regulated RBPs ($\log_2$FC < −0.5; raw $p < .05$ for mouse, *p*-adj < .05 for human) in response to an acute bout of exercise from all four cohorts (mmYS, hsYS, hsAS, and hsAA) were queried, identifying 72 genes (57 were upregulated and 15 were downregulated, across all four groups). The mmYS cohort had 8 and 3 RBPs were significantly up- and down-regulated, respectively, in response to acute exercise. The hsYS cohort had a total of 11 and 1 RBPs were significantly up- and down-regulated, respectively, in response to acute exercise. The hsAS cohort had a total of 39 and 6 RBPs were significantly up- and down-regulated, respectively, in response to acute

exercise. The hsAA cohort had a total of 23 and 5 RBPs were significantly up- and down-regulated, respectively, in response to acute exercise. These genes were subsequently categorized into the following categories: traditional RBPs, hnRNPs & splicing factors, RNA metabolism, RNA helicase, and non-traditional RBPs (Figure 3). Raw *p* values were used to filter mmYS as all 11 included genes did not have significant *p*-adj, except *Sf3b1* ($\log_2$FC = 1.1400, *p*-adj = 0.0336). Overall, these data indicate that acute endurance exercise results in DGE of some RBPs in young organisms, the response of RBPs is much more robust in older individuals.

### 3.3 SRS identified differential splicing events in acutely exercised young and aged skeletal muscle with and without training

Isoform switching, or differential isoform usage (dIF), analyses in human skeletal muscles following acute exercise was first attempted with IsoformSwitchAnalyzeR. Firstly, dIF revealed the most common AS event type of each human cohort (Figure S2A–F). Isoform switching was also determined: compared to the respective baselines, 10 genes had significant isoform-switching events in hsYS, 15 in hsAS, and 21 in hsAA from an acute bout of exercise (Figure S2G).

Subsequently, potential changes in splicing events at the exon level were analyzed with rMATS. The most common event across all three cohorts was SE followed by RI. The hsYS cohort revealed 67 SE events (53.2% of total events, Figure 4A); the hsAS revealed 253 SE events (38.4% of total events, Figure 4B); the hsAA revealed 217 SE events (42.6% of total events, Figure 4C); all with statistical significance (*p*-adj < .05). When comparing the ratio of splicing event types between the younger humans and the older humans, it is interesting to note that exercise induced more A5SS and A3SS in older individuals compared to younger. Also, these data illustrated a considerable difference in number of splicing events in skeletal muscle

between the younger and aged cohorts (younger cohort had 126 total events compared to greater than 300 events in both aged cohorts). Overall, exercise impacts differential exon usage, especially SE events, whereby age and exercise appear to interact to modify differential exon usage to a greater extent.

Genes with statistically significant differential splicing events ($\Delta\Psi > 10\%$, $p$-adj $< .05$) revealed significant GO terms with DAVID functional enrichment analysis (top 10 GO terms illustrated in Figure S3A–C), predominantly pointing out protein binding (GO:0005515), nucleus (GO:0005634), cytoplasm (GO:0005737), RNA/DNA binding (GO:0003723/GO:0003677), ATP binding (GO:0005524), and mitochondrion (GO:0005739). The genes with statistically significant differential splicing events were also compared to observe any overlaps (Figure 4D). Out of 86, 341, and 272 known genes (unique gene IDs; some genes had multiple splicing events, but each gene ID was only entered once in the overlap analysis) from the hsYS, hsAS, and hsAA cohorts respectively, 4 (0.6%) overlapped between hsYS and hsAS, 3 (0.5%) between hsYS and hsAA, 37 (5.7%) between hsAS and hsAA, and 1 (0.2%) across all. A bivariate hypergeometric test between hsAS and hsAA cohorts revealed significant over-enrichment compared to expectations (5.34-fold, $p = 4.606e^{-17}$). Furthermore, genes with significant SE events from these cohorts revealed additional GO terms with the functional enrichment analysis (Figure S3D–F), such as methylation (GO:0032259), ribonucleoprotein complex (GO:1990904), and protein transport (GO:0015031).

### 3.4 LRS identified differential gene expression, differential alternative splicing, and isoform switching in young mice during recovery from acute exercise

Significant DGE and DAS (SE and RI only) of gastrocnemius in mmYS were analyzed using Swan ($\log_2 FC \neq 0$, $\Delta\Pi > 10\%$, raw $p < .05$) to contrast how expressional changes of

transcription and AS differed across the three time points in recovery from acute exercise. Based on mean normalized counts, mmYS-ipe compared to mmYS-pre illustrated DGE only (304, 63.2%), DAS only (143, 29.7%), both DGE and DAS (34, 7.1%) profiles (Figure 5A); mmYS-1pe compared to mmYS-pre illustrated DGE only (231, 66.6%) DAS only (80, 23.1%) both DGE and DAS (36, 10.4%) profiles (Figure 5B); and mmYS-24pe compared to mmYS-pre illustrated DGE only (216, 61.7%), DAS only (107, 30.6%), both DGE and DAS (27, 7.7%) profiles (Figure 5C). These data indicate that exercise not only perturbs transcript expression but also impacts DAS in combination with transcriptional changes and independent of transcriptional changes. This reveals a new source of exercise induced responses and adaptations that need to be explored for their functional relevance in physiology of skeletal muscle and in their roles in exercise induced health benefits.

Isoform switching in gastrocnemius of mmYS-ipe, mmYS-1pe, and mmYS-24pe compared to mmYS-pre was analyzed with Swan. A total of 672, 1094, and 884 transcripts had significant isoform switching events ($\Delta\Pi > 10\%$, $p$-adj $< .05$) at each timepoint, respectively (Figure 5D). Furthermore, 156 (10.1%) overlapped between mmYS-ipe and mmYS-1pe, 114 (7.4%) between mmYS-ipe and mmYS-24pe, 243 (15.7%) between mmYS-1pe and mmYS-24pe, and 295 (19.1%) across all three groups (Figure 5E). When unique gene identifiers of significant isoform-switching genes at each time point were queried (mmYS-ipe = 612, mmYS-1pe = 1009, and mmYS-24pe = 805 genes) for enriched pathways, enrichment of GO terms predominantly included RNA splicing using PANTHER (top 10 GO terms are shown in Figure S4A–C). The 295 common genes across time points post-exercise were independently queried for enriched pathways, revealing enrichment of GO terms including RNA splicing, mRNA processing, and mRNA splicing via spliceosome (top 10 GO terms are shown in Figure 5F).

Within these 295 common genes, 38 were RBPs as identified by overlapping the 295 gene identifiers with a list of 1135 RBP genes generated in house (Figure 5G) and hypergeometric testing revealed that this was significantly over-enriched compared to expectations (fold-change = 2.5, $p = 2.7e^{-7}$).

We visualized the structures of AS transcript variants of the 38 RBPS across pre- and post-exercise time points using Swan. The RBPs were then categorized based on the types of exercise-induced isoform switching (identified from ENSEMBL genome browser transcript identifiers) (Table 1): 11 genes had RI to protein-coding RNA (pcRNA); 9 had complex (ie, multiple types of changes); 8 had pcRNA to pcRNA; 2 had pcRNA to RI; 2 had known to potentially novel transcript variants; 2 had zero pcRNA to pcRNA; 1 had pcRNA to zero or less pcRNA; 1 had potentially novel to known variants; 1 had pcRNA to premature termination codon-containing transcript (bound for RNA decay); and 1 had RI to potentially novel variants.

We also investigated our isoform switching data for known exercise associated genes. We generated a list of 37 well-established exercise-associated genes and overlapped with the list of genes that had significant isoform-switching events at each time point. We observed isoform switching in 22 of those 37 genes (46%) including myosin heavy chain IIX (*Myh4*) and IIA (*Myh2*), *Myc*, *Nr4a1*, and *Mef2c* (Figure S6A–V). These data indicate that in addition to RBPs, that genes that are associated with exercise responses and adaptations also undergo isoform switching events that may be important to investigate their physiological relevance in future mechanistic follow up studies.

## 3.5 Validation of hnRNPA3 isoform switching and protein expression across timepoints post exercise

Among the isoform-switching RBPs, *Hnrnpa3* had a splicing profile with biological significance according to the LRS data (Figure 6A,B). It was evident that a RI variant (*Hnrnpa3*-205) was dominant at baseline (mmYS-pre), there was a complete switch post-exercise (mmYS-ipe and -1pe), whereby the pcRNA variants (*Hnrnpa3*-203/-204) become the dominant forms. At the 24-hour time point, the proportions of the mRNA transcript variants were split 50% between RI (-205) and pcRNA (-204). Protein levels were determined for hnRNP-A3 to validate this isoform-switching event (Figure 6C). HnRNP-A3 was detectable at baseline according to the western blots, one-way ANOVA revealed statistical difference between the pre- and post-exercise time points ($F = 6.872$, $p = 0.0035$). *Post hoc* comparisons revealed no statistical difference between mmYS-pre and mmYS-ipe (23.1% increase, $p$-adj = 0.6876), but was found significant for mmYS-1pe and mmYS-24pe (95.6% and 84.9% increases, $p$-adj = 0.0043 and 0.0103, respectively).

## 4 DISCUSSION

The present study supports that, in addition to DGE in recovery from endurance exercise, there is a robust AS response across the transcriptome. Our data indicate that while some RBPs and spliceosome proteins undergo DGE in response to an acute bout of endurance exercise in untrained skeletal muscle, far more RBPs and spliceosome proteins undergo DAS and isoform switching in response to exercise. Our rMATS analysis of SRS data revealed that young individuals have splicing events in response to endurance exercise, but both sedentary and trained older individuals have a greater number of events detected compared to younger individuals. While SRS is excellent for detecting DGE and exon splicing events, it lacks the resolution to accurately detect transcript variants and/or isoform-switching events due to multi-read alignment and mapping ambiguity.[47] Finally, our data clearly points out the strengths of LRS for the detection of full-length transcript variants and opens an entirely new area of adaptive potential in skeletal muscle to explore in response to endurance exercise.

Recent literature has indicated changes in the expression of transcript variants with aging in skeletal muscle.[16,48–52] Since endurance exercise is a potent anti-aging intervention (ie, by maintaining $V\square O_2max$), we surmised that the response of skeletal muscle gene expression at the level of AS would differ by age and training status. Our data clearly indicate that this is likely the case (Figure 3,4). First, since previous research has shown significant RNA and protein level differences in RBPs with age, we explored a biased DGE analysis of RBPs. This revealed that acute endurance exercise in young individuals had a minimal impact on DGE of RBPs in comparison to the effect acute endurance exercise in muscles of older individuals (Figure 3). Interestingly, older trained individuals had fewer differentially expressed RBPs in response to acute exercise compared to acute exercise in sedentary individuals (Figure 3). This finding is in

line with recently published data that indicated lower RBP expression levels in masters athletes compared to age-matched non-athletes.[53]

Becoming or remaining physically active, as well as performing regular exercise, shifts to play a more important role in health as one ages than during their youth. Recent findings have indicated that AS becomes dysregulated with aging in several tissues, including skeletal muscle.[16,54] When aged skeletal muscles were compared to younger muscles, proteins of the spliceosome and several RBPs were overrepresented, leading to a change in the expressed variants of mRNA.[16] Interestingly, when octogenarian masters athletes were compared to age-matched non-athletes, the athletes had lower protein expression of the spliceosomal and several RBPs.[53] The authors went on to hypothesize that the underrepresentation of the spliceosomal proteins was related to the higher functioning mitochondria and the lower need for energy to be expended for splice-isoform generation.[53] Thus, further research is needed to link exercise, AS regulation, and mRNA variant generation to the adaptive process in skeletal muscle of both younger and older adults.

Next, we used rMATS to explore the type and number of AS events at the exon level from the SRS from humans (Figure 4). To our knowledge, rMATS has not previously been used to explore how exercise may modify AS, allowing us to make several novel insights. Collectively, it is apparent that SE is the dominant form of alternative splicing event category in response to an acute bout of exercise while A5SS and A3SS are potentially subjected to other factors, such as age. The second most abundant type of splicing event across all data sets was RI (Figure 4). Both SE and RI events have important implications on the transcriptome and proteome that should be explored in future studies, but these data provide novel mechanistic insights into how acute endurance exercise is modifying gene expression and potentially skeletal

muscle responses and adaptations to exercise. Second, we observed that there were fewer splicing events in the muscles of younger individuals compared to older individuals in response to exercise. However, we interpret this cautiously due to technical limitations and differences with how the samples were collected and the way the sequencing was performed between the data sets. Future studies will be needed to test this important question more carefully. A third observation is that older skeletal muscles utilized more A5SS and A3SS compared to younger muscles in response to a bout of endurance exercise. This could be due to the different responses of signal transduction pathways to modify the splicing machinery in older muscles compared to younger muscles. Alternatively, this could indicate a greater energetic stress in older muscles leading to different signaling pathways being activated, resulting in the utilization of weaker splice sites. This could have important ramifications on the transcriptome and proteome following exercise in older muscles and should be explored in more detail in future research.[55,56]

While SRS is a powerful technology and our data above illustrate its ability to detect DGE and exon level splicing events, it lacks the ability to detect full-length transcripts, which have great implications on the expression of protein isoforms. Thus, we next wanted to determine if additional insights could be made concerning how exercise mechanistically impacts skeletal muscle by using LRS. First, we were able to separate DGE and DAS using the LRS data (Figure 5A–C). This revealed that a significant portion of genes only undergo DAS, meaning previous post-exercise DGE analyses would not have detected these changes even though they would have likely impacted the post-exercise protein levels in muscle. Next, we analyzed isoform switching, specifically in genes that were not differentially expressed following exercise. We observed a robust isoform-switching response at all three time points in recovery from endurance exercise (Figure 5D). Further analysis illuminated a significant enrichment of RBPs

that undergo isoform-switching events during recovery from endurance exercise (Figure 5E–G). In other words, RBPs and splicing factors undergo regulatory alteration by genes encoding these proteins via AS. Such regulatory process is referred to as either auto-regulation (whereby a RBP regulates the splicing of its own transcripts) or cross-regulation (whereby a RBP regulates the splicing of other RBP-coding transcripts). This idea of auto- and cross-regulation as a means of regulating functional levels of RBPs is not a novel concept in the field of RNA biology, as previously demonstrated in neuronal (NOVA1)[57] and cancer (PTBP1/2 and SRSF3)[58] cells.

Interestingly, several of the isoform-switching events lasted at least 24 hours into recovery from exercise, indicating a lasting (ie, not transient) re-wiring of the transcriptome that likely impacts the proteome as we have shown is the case for hnRNP-A3 (Figure 6A–C). Splicing and AS are regulated by a multitude of factors including (but not limited to) transcriptional rate, chromatin structure, the spliceosome, and RBPs.[4,5] The potential for exercise to modify the activity of the spliceosome, as well as post-translational modification of RBPs which may impact binding to their respective target RNAs (and thus modify their splicing), is particularly important. RBPs bind to RNAs and impact their entire lifecycle: from splicing to localization, to translation, and degradation.[18] Specifically, RBPs bind to *cis*-regulatory elements (ie, intronic/exonic splicing enhancers and silencers) to regulate the inclusion of specific exons, resulting in the expression of different transcript variants and protein isoforms. Differential use of isoforms between conditions (isoform switching) can have profound biological impacts, even if they are only transiently induced by exercise, due to the difference in functions of the isoforms. Functional consequences of isoform switches can include gain or loss of protein domains or signal peptides, loss of protein coding sequence, and change in propensity for nonsense-mediated decay.[13] Isoform switches are implicated in many diseases, and it has already been observed

following exercise (PGC-1α),[15] however the full extent and impact of isoform switching post-exercise is far from understood.

It is highly likely, but not yet tested, that exercise remodels the binding patterns of RBPs either through post-translational modifications (PTMs) of the RBPs themselves or through isoform switching and AS changes to RBPs themselves, which would modify the target genes of RBPs. Metabolic stress responsive pathways, such as AMPK, are already known to regulate PTMs of RBPs.[21] Interestingly, many RBPs tend to regulate their protein abundance through AS and isoform switching. Our isoform switching data indicate an enrichment of events in RBPs post-exercise. This indicates that exercise may remodel the expression of protein isoforms by modifying the function of RBPs. Our findings not only support the preceding study from our laboratory that focused on SF3B4 and SRSF2,[29] but others that have observed similar phenomenon in a separate setting: Henrich et al[59] illustrated 9 weeks of microgravity conditions leading to AS-driven diversification of the transcriptome in mouse skeletal muscle, including RBPs (eg, *Mbnl1* and *Rbfox1*). This mechanism is important in shaping the transcriptome and proteome in response to specific cellular stresses. Bringing this idea to the study of skeletal muscle adaptations in response to exercise is an innovative and novel molecular mechanism of adaptation (Figure 7).

The present study is not without limitations. The human SRS data utilized for this study included on average 20 million reads per sample, which is insufficient/minimum threshold to yield biologically true isoform-switching analyses with IsoformSwitchAnalyzeR. Hence, there is a growing need for employing LRS technologies to better examine alternative splicing and isoform switching in the field of exercise biology. Additionally, the mice cohort had mixed sexes unlike the human cohorts utilized for analyses, which may further limit the comparability. Indeed,

protein analysis was only conducted for our candidate RBP, hnRNP-A3, but not at the global level for this study. To better validate the significance of DAS and isoform-switching events, future studies will incorporate proteomics data with these LRS data via proteogenomic approaches.

In summary, the present data supports recent evidence of divergence in the skeletal muscle AS-related responses and RBP expression by age and training status. Moreover, LRS is the preferrable method of transcriptomics study when exploring AS and isoform-switching events, whereas utilizing SRS may require cost prohibitive read depth per sample for many groups (at least 100 million reads per sample) to proficiently conduct the isoform switching analyses. Additionally, our acute endurance exercise mouse model demonstrated that, even without any changes in overall gene expression, the protein expression of hnRNP-A3 was increased by nearly two-fold in response to exercise for at least 24 hours via isoform switching with the power of LRS. Therefore, our study points out that AS following exercise in skeletal muscle is an underexplored and untapped area of ripe to increase our mechanistic understanding of exercise.

## IV: DATA AVAILABILITY STATEMENT

The human SRS data were extracted from deposits by Pattamaprapanont et al[30] and Rubenstein et al[31] in the NCBI Gene Expression Omnibus database with the accession numbers GSE87749 and GSE151066, respectively. The mouse LRS data are deposited in the NCBI Gene Expression Omnibus database with the accession number GSE279359. All data used to generate the figures in this manuscript will be deposited at the Deep Blue Data repository with a permanent DOI (DOI will be provided upon publication).

## V: CONFLICT OF INTEREST STATEMENT

The authors declare that the research was conducted in the absence of any commercial or financial relationships that could be construed as a potential conflict of interest. The authors declare no competing interests.

## VI: AUTHOR CONTRIBUTIONS

AA, ALS, JJK, and ATL conceived and/or designed the research. AA, ALS, JJK performed the research and acquired the data, AA, JJK, JYY, EYZ, and ATL analyzed and interpreted the data. All authors were involved in drafting and revising the manuscript.

## VII: ACKNOWLEDGMENTS

This research was supported by the National Institutes of Health and National Cancer Institute under award number 5R00CA197672-04, Michigan Integrative Musculoskeletal Health Core Center (MiMHC) P30 grant from NIH/NIAMS under award number P30 AR069620, and the University of Michigan's School of Kinesiology Marie Hartwig Research Fund.

# VIII: REFERENCES

1. CDC. Adult Physical Inactivity. Centers for Disease Control and Prevention. November 20, 2023. Accessed February 3, 2024. https://www.cdc.gov/physicalactivity/data/inactivity-prevalence-maps/index.html

2. Lee IM, Shiroma EJ, Lobelo F, et al. Effect of physical inactivity on major non-communicable diseases worldwide: an analysis of burden of disease and life expectancy. *Lancet*. 2012;380(9838):219-229. doi:10.1016/S0140-6736(12)61031-9

3. Holloszy JO, Smith EK, Vining M, Adams S. Effect of voluntary exercise on longevity of rats. *Journal of Applied Physiology*. 1985;59(3):826-831. doi:10.1152/jappl.1985.59.3.826

4. Tomasek JJ, Gabbiani G, Hinz B, Chaponnier C, Brown RA. Myofibroblasts and mechano-regulation of connective tissue remodelling. *Nat Rev Mol Cell Biol*. 2002;3(5):349-363. doi:10.1038/nrm809

5. Ferraro E, Giammarioli AM, Chiandotto S, Spoletini I, Rosano G. Exercise-Induced Skeletal Muscle Remodeling and Metabolic Adaptation: Redox Signaling and Role of Autophagy. *Antioxid Redox Signal*. 2014;21(1):154-176. doi:10.1089/ars.2013.5773

6. Powers SK, Talbert EE, Adhihetty PJ. Reactive oxygen and nitrogen species as intracellular signals in skeletal muscle. *J Physiol*. 2011;589(Pt 9):2129-2138. doi:10.1113/jphysiol.2010.201327

7. Egan B, Sharples AP. Molecular responses to acute exercise and their relevance for adaptations in skeletal muscle to exercise training. *Physiological Reviews*. 2023;103(3):2057-2170. doi:10.1152/physrev.00054.2021

8. Pillon NJ, Gabriel BM, Dollet L, et al. Transcriptomic profiling of skeletal muscle adaptations to exercise and inactivity. *Nat Commun*. 2020;11(1):470. doi:10.1038/s41467-019-13869-w

9. Amar D, Lindholm ME, Norrbom J, Wheeler MT, Rivas MA, Ashley EA. Time trajectories in the transcriptomic response to exercise - a meta-analysis. *Nat Commun*. 2021;12(1):3471. doi:10.1038/s41467-021-23579-x

10. Mathai AS, Bonen A, Benton CR, Robinson DL, Graham TE. Rapid exercise-induced changes in PGC-1α mRNA and protein in human skeletal muscle. *Journal of Applied Physiology*. 2008;105(4):1098-1105. doi:10.1152/japplphysiol.00847.2007

11. Gustafsson T, Puntschart A, Kaijser L, Jansson E, Sundberg CJ. Exercise-induced expression of angiogenesis-related transcription and growth factors in human skeletal muscle. *American Journal of Physiology-Heart and Circulatory Physiology*. 1999;276(2):H679-H685. doi:10.1152/ajpheart.1999.276.2.H679

12. Gahlmann R, Troutt AB, Wade RP, Gunning P, Kedes L. Alternative splicing generates variants in important functional domains of human slow skeletal troponin T. *Journal of Biological Chemistry*. 1987;262(33):16122-16126. doi:10.1016/S0021-9258(18)47705-8

13. Norrbom J, Sällstedt EK, Fischer H, Sundberg CJ, Rundqvist H, Gustafsson T. Alternative splice variant PGC-1α-b is strongly induced by exercise in human skeletal muscle. *American Journal of Physiology-Endocrinology and Metabolism*. 2011;301(6):E1092-E1098. doi:10.1152/ajpendo.00119.2011

14. Jensen L, Pilegaard H, Neufer PD, Hellsten Y. Effect of acute exercise and exercise training on VEGF splice variants in human skeletal muscle. *Am J Physiol Regul Integr Comp Physiol*. 2004;287(2):R397-402. doi:10.1152/ajpregu.00071.2004

15. Zhang T, Choi SJ, Wang ZM, et al. Human Slow Troponin T (TNNT1) Pre-mRNA Alternative Splicing Is an Indicator of Skeletal Muscle Response to Resistance Exercise in Older Adults. *The Journals of Gerontology: Series A*. 2014;69(12):1437-1447. doi:10.1093/gerona/glt204

16. Ubaida-Mohien C, Gonzalez-Freire M, Lyashkov A, et al. Physical Activity Associated Proteomics of Skeletal Muscle: Being Physically Active in Daily Life May Protect Skeletal Muscle From Aging. *Front Physiol*. 2019;10:312. doi:10.3389/fphys.2019.00312

17. Innocenzi E, Cariati I, De Domenico E, et al. Aerobic Exercise Induces Alternative Splicing of Neurexins in Frontal Cortex. *J Funct Morphol Kinesiol*. 2021;6(2):48. doi:10.3390/jfmk6020048

18. Wahl MC, Will CL, Lührmann R. The Spliceosome: Design Principles of a Dynamic RNP Machine. *Cell*. 2009;136(4):701-718. doi:10.1016/j.cell.2009.02.009

19. Tao Y, Zhang Q, Wang H, Yang X, Mu H. Alternative splicing and related RNA binding proteins in human health and disease. *Sig Transduct Target Ther*. 2024;9(1):1-33. doi:10.1038/s41392-024-01734-2

20. Anczukow O, Allain FHT, Angarola BL, et al. Steering research on mRNA splicing in cancer towards clinical translation. *Nat Rev Cancer*. Published online October 9, 2024:1-19. doi:10.1038/s41568-024-00750-2

21. Tao Y, Zhang Q, Wang H, Yang X, Mu H. Alternative splicing and related RNA binding proteins in human health and disease. *Sig Transduct Target Ther*. 2024;9(1):1-33. doi:10.1038/s41392-024-01734-2

22. Aebersold R, Agar JN, Amster IJ, et al. How many human proteoforms are there? *Nat Chem Biol*. 2018;14(3):206-214. doi:10.1038/nchembio.2576

23. Manuel JM, Guilloy N, Khatir I, Roucou X, Laurent B. Re-evaluating the impact of alternative RNA splicing on proteomic diversity. *Frontiers in Genetics*. 2023;14. Accessed February 9, 2024. https://www.frontiersin.org/journals/genetics/articles/10.3389/fgene.2023.1089053

24. Dinger ME, Amaral PP, Mercer TR, et al. Long noncoding RNAs in mouse embryonic stem cell pluripotency and differentiation. *Genome Res*. 2008;18(9):1433-1445. doi:10.1101/gr.078378.108

25. Khan MR, Avino M, Wellinger RJ, Laurent B. Distinct regulatory functions and biological roles of lncRNA splice variants. *Molecular Therapy - Nucleic Acids*. 2023;32:127-143. doi:10.1016/j.omtn.2023.03.004

26. Saudemont B, Popa A, Parmley JL, et al. The fitness cost of mis-splicing is the main determinant of alternative splicing patterns. *Genome Biol*. 2017;18(1):208. doi:10.1186/s13059-017-1344-6

27. García-Moreno JF, Romão L. Perspective in Alternative Splicing Coupled to Nonsense-Mediated mRNA Decay. *Int J Mol Sci*. 2020;21(24):9424. doi:10.3390/ijms21249424

28. Tonevitsky EA, Trushkin EV, Shkurnikov MU, Akimov EB, Sakharov DA. Changed Profile of Expression of Splicing Regulator Genes in Response to Exercise. *Bull Exp Biol Med*. 2009;147(6):733-736. doi:10.1007/s10517-009-0593-0

29. Slusher AL, Kim JJ, Ribick M, Ludlow AT. Acute Exercise Regulates hTERT Gene Expression and Alternative Splicing in the hTERT-BAC Transgenic Mouse Model. *Med Sci Sports Exerc*. 2022;54(6):931-943. doi:10.1249/mss.0000000000002868

30. Pattamaprapanont P, Garde C, Fabre O, Barrès R. Muscle Contraction Induces Acute Hydroxymethylation of the Exercise-Responsive Gene Nr4a3. *Front Endocrinol (Lausanne)*. 2016;7:165. doi:10.3389/fendo.2016.00165

31. Rubenstein AB, Hinkley JM, Nair VD, et al. Skeletal muscle transcriptome response to a bout of endurance exercise in physically active and sedentary older adults. *American Journal of Physiology-Endocrinology and Metabolism*. 2022;322(3):E260-E277. doi:10.1152/ajpendo.00378.2021

32. Fernando P, Bonen A, Hoffman-Goetz L. Predicting submaximal oxygen consumption during treadmill running in mice. *Can J Physiol Pharmacol*. 1993;71(10-11):854-857. doi:10.1139/y93-128

33. Li B, Dewey CN. RSEM: accurate transcript quantification from RNA-Seq data with or without a reference genome. *BMC Bioinformatics*. 2011;12(1):323. doi:10.1186/1471-2105-12-323

34. Dobin A, Davis CA, Schlesinger F, et al. STAR: ultrafast universal RNA-seq aligner. *Bioinformatics*. 2013;29(1):15-21. doi:10.1093/bioinformatics/bts635

35. Li H. Minimap2: pairwise alignment for nucleotide sequences. *Bioinformatics*. 2018;34(18):3094-3100. doi:10.1093/bioinformatics/bty191

36. Danecek P, Bonfield JK, Liddle J, et al. Twelve years of SAMtools and BCFtools. *GigaScience*. 2021;10(2):giab008. doi:10.1093/gigascience/giab008

37. Wyman D, Mortazavi A. TranscriptClean: variant-aware correction of indels, mismatches and splice junctions in long-read transcripts. *Bioinformatics*. 2019;35(2):340-342. doi:10.1093/bioinformatics/bty483

38. Wyman D, Balderrama-Gutierrez G, Reese F, et al. A technology-agnostic long-read analysis pipeline for transcriptome discovery and quantification. Published online March 24, 2020:672931. doi:10.1101/672931

39. Soneson C, Love MI, Robinson MD. Differential analyses for RNA-seq: transcript-level estimates improve gene-level inferences. Published online February 29, 2016. doi:10.12688/f1000research.7563.2

40. Love MI, Huber W, Anders S. Moderated estimation of fold change and dispersion for RNA-seq data with DESeq2. *Genome Biology*. 2014;15(12):550. doi:10.1186/s13059-014-0550-8

41. Vitting-Seerup K, Sandelin A. IsoformSwitchAnalyzeR: analysis of changes in genome-wide patterns of alternative splicing and its functional consequences. *Bioinformatics*. 2019;35(21):4469-4471. doi:10.1093/bioinformatics/btz247

42. Shen S, Park JW, Lu Z xiang, et al. rMATS: Robust and flexible detection of differential alternative splicing from replicate RNA-Seq data. *Proc Natl Acad Sci U S A.* 2014;111(51):E5593-E5601. doi:10.1073/pnas.1419161111

43. Wang Y, Xie Z, Kutschera E, Adams JI, Kadash-Edmondson KE, Xing Y. rMATS-turbo: an efficient and flexible computational tool for alternative splicing analysis of large-scale RNA-seq data. *Nat Protoc*. Published online February 23, 2024:1-22. doi:10.1038/s41596-023-00944-2

44. Reese F, Mortazavi A. Swan: a library for the analysis and visualization of long-read transcriptomes. *Bioinformatics*. 2021;37(9):1322-1323. doi:10.1093/bioinformatics/btaa836

45. Sherman BT, Hao M, Qiu J, et al. DAVID: a web server for functional enrichment analysis and functional annotation of gene lists (2021 update). *Nucleic Acids Research.* 2022;50(W1):W216-W221. doi:10.1093/nar/gkac194

46. Thomas PD, Ebert D, Muruganujan A, Mushayahama T, Albou LP, Mi H. PANTHER: Making genome-scale phylogenetics accessible to all. *Protein Science*. 2022;31(1):8-22. doi:10.1002/pro.4218

47. Slotkin RK. The case for not masking away repetitive DNA. *Mob DNA*. 2018;9:15. doi:10.1186/s13100-018-0120-9

48. Ubaida-Mohien C, Lyashkov A, Gonzalez-Freire M, et al. Discovery proteomics in aging human skeletal muscle finds change in spliceosome, immunity, proteostasis and mitochondria. Kaeberlein M, Rosen CJ, Kaeberlein M, Anderson R, eds. *eLife*. 2019;8:e49874. doi:10.7554/eLife.49874

49. Solovyeva EM, Ibebunjo C, Utzinger S, et al. New insights into molecular changes in skeletal muscle aging and disease: Differential alternative splicing and senescence. *Mechanisms of Ageing and Development*. 2021;197:111510. doi:10.1016/j.mad.2021.111510

50. Rodríguez SA, Grochová D, McKenna T, et al. Global genome splicing analysis reveals an increased number of alternatively spliced genes with aging. *Aging Cell*. 2016;15(2):267-278. doi:10.1111/acel.12433

51. Tumasian RA, Harish A, Kundu G, et al. Skeletal muscle transcriptome in healthy aging. *Nat Commun*. 2021;12(1):2014. doi:10.1038/s41467-021-22168-2

52. Lee BP, Pilling LC, Emond F, et al. Changes in the expression of splicing factor transcripts and variations in alternative splicing are associated with lifespan in mice and humans. *Aging Cell*. 2016;15(5):903-913. doi:10.1111/acel.12499

53. Ubaida-Mohien C, Spendiff S, Lyashkov A, et al. Unbiased proteomics, histochemistry, and mitochondrial DNA copy number reveal better mitochondrial health in muscle of high-functioning octogenarians. Grano M, Isales C, Piasecki M, Degens H, eds. *eLife*. 2022;11:e74335. doi:10.7554/eLife.74335

54. Angarola BL, Anczuków O. Splicing alterations in healthy aging and disease. *Wiley Interdiscip Rev RNA*. 2021;12(4):e1643. doi:10.1002/wrna.1643

55. Bartz J, Jung H, Wasiluk K, Zhang L, Dong X. Progress in Discovering Transcriptional Noise in Aging. *International Journal of Molecular Sciences*. 2023;24(4):3701. doi:10.3390/ijms24043701

56. Perez-Gomez A, Buxbaum JN, Petrascheck M. The aging transcriptome: read between the lines. *Current Opinion in Neurobiology*. 2020;63:170-175. doi:10.1016/j.conb.2020.05.001

57. Dredge BK, Stefani G, Engelhard CC, Darnell RB. Nova autoregulation reveals dual functions in neuronal splicing. *EMBO J*. 2005;24(8):1608-1620. doi:10.1038/sj.emboj.7600630

58. Guo J, Jia J, Jia R. PTBP1 and PTBP2 impaired autoregulation of SRSF3 in cancer cells. *Sci Rep*. 2015;5(1):14548. doi:10.1038/srep14548

59. Henrich M, Ha P, Wang Y, et al. Alternative splicing diversifies the skeletal muscle transcriptome during prolonged spaceflight. *Skelet Muscle*. 2022;12:11. doi:10.1186/s13395-022-00294-9

# IX: FIGURE LEGENDS

**Figure 1.** Layout of RNA-Seq study. (A) Publicly accessible human SRS data (hsYS, hsAS, and hsAA) were downloaded from NCBI Gene Expression Omnibus, preprocessed, and analyzed for differential expression. (B) Young C57BL/6 mice (mmYS) underwent an acute bout (30 minutes) of treadmill running, sacrificed, and their gastrocnemius skeletal muscle tissues were harvested for RNA sequencing cDNA library prep. Following LRS, the data were preprocessed and analyzed for differential expression. Biologically significant genes from (A) and (B) were retrieved for subsequent pathway and biased analyses.

**Figure 2.** Differential gene expression (DGE) of hsYS (A-C), hsAS (D,E), hsAA (F,G), and mmYS (H-J) in the skeletal muscle comparing pre- and post-acute exercise. (A) Volcano plot of hsYS-pre and hsYS-4pe DGE. (B) Top 10 GO terms from significantly up-regulated genes of hsYS-pre and hsYS-4pe DGE. (C) Top GO terms from significantly down-regulated genes of hsYS-pre and hsYS-4pe DGE. (D) Volcano plot of hsAS-pre and hsAS-3pe DGE. (E) Top 10 GO terms from significantly up-regulated genes of hsAS-pre and hsAS-3pe DGE. (F) Volcano plot of hsAA-pre and hsAA-3pe DGE. (G) Top 10 GO terms from significantly up-regulated genes of hsAA-pre and hsAA-3pe DGE. (H) Volcano plot of mmYS-pre and mmYS-1pe DGE. (I) Top 10 GO terms from significantly up-regulated genes of mmYS-pre and mmYS-1pe DGE. (J) Top GO terms from significantly down-regulated genes of mmYS-pre and mmYS-1pe DGE.

**Figure 3.** Biased differential gene expression of biologically significant ($|\log_2 FC| > 0.5$; raw $p < .05$ for mouse, $p$-adj $< .05$ for human) RNA-binding proteins in response to an acute bout of exercise in skeletal muscle with and without training. The 72 genes were binned to one of traditional RBPs, hnRNPs & splicing factors, RNA metabolism, RNA helicase, and non-traditional RBPs.

**Figure 4.** Differential splicing events in acutely exercised young and aged skeletal muscle with and without training. (A) Level of potential splicing change detected between hsYS-pre and hsYS-4pe, categorized into 5 common event types (SE, RI, MXE, A5SS, and A3SS). (B) Level of potential splicing change detected between hsAS-pre and hsAS-3pe, categorized into 5 common event types. (C) Level of potential splicing change detected between hsAA-pre and hsAA-3pe, categorized into 5 common event types. (D) Euler overlap of genes with differences in potential splicing events detected pre- and post-acute exercise across the three human SRS cohorts.

**Figure 5.** Splicing and isoform switching in acutely exercised young sedentary skeletal muscle in a temporal manner. (A) Expressional changes in genes with significant (raw $p < .05$) DGE and DAS between mmYS-pre and mmYS-ipe. (B) Expressional changes in genes with significant DGE and DAS between mmYS-pre and mmYS-1pe. (C) Expressional changes in genes with significant DGE and DAS between mmYS-pre and mmYS-24pe. (D) Isoform switching genes with statistical significance ($\Delta\Pi > 10\%$, $p$-adj $< .05$) between pre- and post-acute exercise time points. (E) Euler overlap of isoform switching genes with statistical significance between pre- and post-acute exercise time points. (F) Top 10 GO terms from the 295 common genes across the three post-acute exercise time points found in Figure 4E. (G) Overlap of the 295 common genes with in-house list of 1135 RBP genes, highlighting significant DAS of 38 RBP genes without significant DGE.

**Figure 6.** Acute bout of treadmill running increased expression of splicing factor hnRNP-A3 in skeletal muscle without training. (A) Transcript expressional and splicing profile of Hnrnpa3 obtained from LRS data, illustrating RI (Hnrnpa3-205) to pcRNA (Hnrnpa3-203/-204) in response to acute exercise. (B) Transcript expressional and splicing profile of Hnrnpa3 in $\Delta\Pi$

from Figure 6A illustrated as a bar chart. (C) Western blot validation of significant isoform switching of hnRNP-A3 at the protein level, normalized to total protein at 40-45 kDa band detection then normalized to mmYS-pre for relative quantification in arbitrary units (AU), included with representative image of western blots. *, p-adj < 0.05 compared to mmYS-pre. **, p-adj < 0.01 compared to mmYS-pre. All experiments were conducted with n = 5 per cohort (Figure S5D).

**Figure 7.** Current model on the effects of acute endurance exercise on the AS regulatory mechanism with key *trans*-factors/RBPs.

# X: TABLES

**Table 1.** Biologically significant RNA-binding proteins selected and categorized based on the types of exercise-induced changes in isoform switching events.

| **Types of exercise-induced changes in isoforms** | RI to pcRNA | Complex to complex | pcRNA to pcRNA | pcRNA to RI | Known to novel transcript | lncRNA to pcRNA | pcRNA to lncRNA/ less pcRNA | Novel transcript to known | pcRNA to NMD | RI to novel transcript |
|---|---|---|---|---|---|---|---|---|---|---|
| **Gene Names** | Eif4g2<br>Hnrnpa3<br>Hnrnpc<br>Mrpl37<br>Mthfsd<br>Noc4l<br>Nosip<br>Rnps1<br>Rpl3<br>Tia1<br>U2af1l4 | Mbnl1<br>Hnrnpa2b1<br>Hnrnpf<br>Rack1<br>Rpl10a<br>Rpl18a<br>Rsrc2<br>Srsf5<br>Srsf7 | Arhgdip<br>Grsf1<br>Ivns1abp<br>Mtpap<br>Ppil3<br>Pqbp1<br>Rps13<br>Snrnpa | Hnrnpr<br>Mphosph | Mbnl2<br>Pfn1 | Dnajc8<br>Rbm39 | Rpl37 | Cpsf4 | Hnrnpa1 | Hnrnpk |
| **Final count** | 11 | 9 | 8 | 2 | 2 | 2 | 1 | 1 | 1 | 1 |

# XI: SUPPLEMENTAL FIGURE LEGENDS

**Figure S1.** RNA-Seq data quality metrics and animal acute treadmill running model. Bar graph of total read count of (A) hsYS, (B) hsAS, (C) hsAA, and (D) mmYS cohort data by sample in millions. Euclidean hierarchical heatmap analysis of (E) hsYS, (F) hsAS, (G) hsAA, and (H) mmYS cohort data by sample. Principal component analysis of (I) hsYS, (J) hsAS, (K) hsAA, and (L) mmYS cohort data by sample. (M) Overview of treadmill acclimation protocol, max speed test, and pre-/post-acute exercise time points of skeletal muscle harvests.

**Figure S2.** Violin plots of genome-wide differences in isoform fraction (IF) across (A) hsYS, (B) hsAS, and (C) hsAA cohorts compared between pre- and post-acute bout of exercise using IsoformSwitchAnalyzeR. Differences in IF revealed enrichment of genes stratified in AS event type across (D) hsYS, (E) hsAS, and (F) hsAA cohorts compared between pre- and post-acute bout of exercise. (G) Isoform switching genes with statistical significance ($\Delta\Pi > 10\%$, *p*-adj $< .05$) between pre- and post-acute exercise time points across the human cohorts. (H) Isoform switching genes with statistical significance and predicted biological outcomes between pre- and post-acute exercise time points across the human cohorts.

**Figure S3.** Differential splicing events of hsYS (A,D), hsAS (B,E), and hsAA (C,F) in the skeletal muscle comparing pre- and post-acute exercise using rMATS. (A) Top 10 GO terms of enriched genes with splicing events of hsYS-pre and hsYS-4pe. (B) Top 10 GO terms of enriched genes with splicing events of hsAS-pre and hsAS-3pe. (C) Top 10 GO terms of enriched genes with splicing events of hsAA-pre and hsAA-3pe. (D) Top 10 GO terms of enriched genes with skipped exons of hsYS-pre and hsYS-4pe. (E) Top 10 GO terms of enriched genes with skipped exons of hsAS-pre and hsAS-3pe. (F) Top 10 GO terms of enriched genes with skipped exons of hsAA-pre and hsAA-3pe.

**Figure S4.** Significant isoform-switching genes and additional DGE data of mmYS in the skeletal muscle comparing pre- and post-acute exercise using Swan. (A) Top 10 GO terms of enriched genes with isoform-switching events of mmYS-pre and mmYS-ipe using PANTHER. (B) Top 10 GO terms of enriched genes with isoform-switching events of mmYS-pre and mmYS-1pe using PANTHER. (C) Top 10 GO terms of enriched genes with isoform-switching events of mmYS-pre and mmYS-24pe using PANTHER. (D) Volcano plot of mmYS-pre and mmYS-ipe DGE. (E) Volcano plot of mmYS-pre and mmYS-24pe DGE.

**Figure S5.** Western blot validation of anti-hnRNP-A3 antibody in human and mouse samples. (A) Wild-type HEK 293 cells were used to verify cross-species specificity of the hnRNP-A3 antibody and was loaded by 50k, 25k, and 10k cells. (B,C) C2C12 myoblasts were transfected with 30 nM of either siCTL or *Hnrnpa3* siRNA for 24 and 48 h to validate protein specificity of the antibody. (D) Full collection of western blots used to analyze significant isoform switching of hnRNP-A3 at the protein level, normalized to total protein at 40-45 kDa band detection then normalized to mmYS-pre for relative quantification in AU. ****, $p < 0.0001$ compared to siCTL.

**Figure S6.** Transcript expressional and splicing profile of 22 well-established exercise-associated genes with significant isoform switching obtained from LRS data. (A) Myelocytomatosis oncogene; *Myc*. (B) Nuclear receptor subfamily 4, group A, member 1; *Nr4a1*. (C) Pyruvate dehydrogenase kinase, isoenzyme 4; *Pdk4*. (D) Sirtuin 2; *Sirt2*. (E) Sirtuin 3; *Sirt3*. (F) Sirtuin 5; *Sirt5*. (G) Heat shock protein 5; *Hspa5*. (H) Heat shock protein 70 family, member 13; *Hspa13*. (I) Heat shock protein 70 family, member 11; *Hspa11*. (J) Insulin-like growth factor 1; *Igf1*. (K) Insulin-like growth factor 2; *Igf2*. (L) Interlukin-11 receptor subunit α 1; *Il11ra1*. (M) Interlukin-15 receptor, α chain; *Il15ra*. (N) Interlukin-33; *Il33*. (O) Muscleblind-like splicing regulator 1; *Mbnl1*. (P) Muscleblind-like splicing regulator 2; *Mbnl2*. (Q) Myocyte enhancer

factor 2C; *Mef2c*. (R) Mitochondrial transcription termination factor; *Mterf2*. (S) Myosin, heavy polypeptide 2, skeletal muscle, adult; MYH type IIA; *Myh2*. (T) Myosin, heavy polypeptide 4, skeletal muscle, adult; MYH type IIX; *Myh4*. (U) Heat shock protein 2; *Hspb2*. (V) Nuclear receptor subfamily 2, group F, member 2; *Nr2f2*.

**Figure 1.**

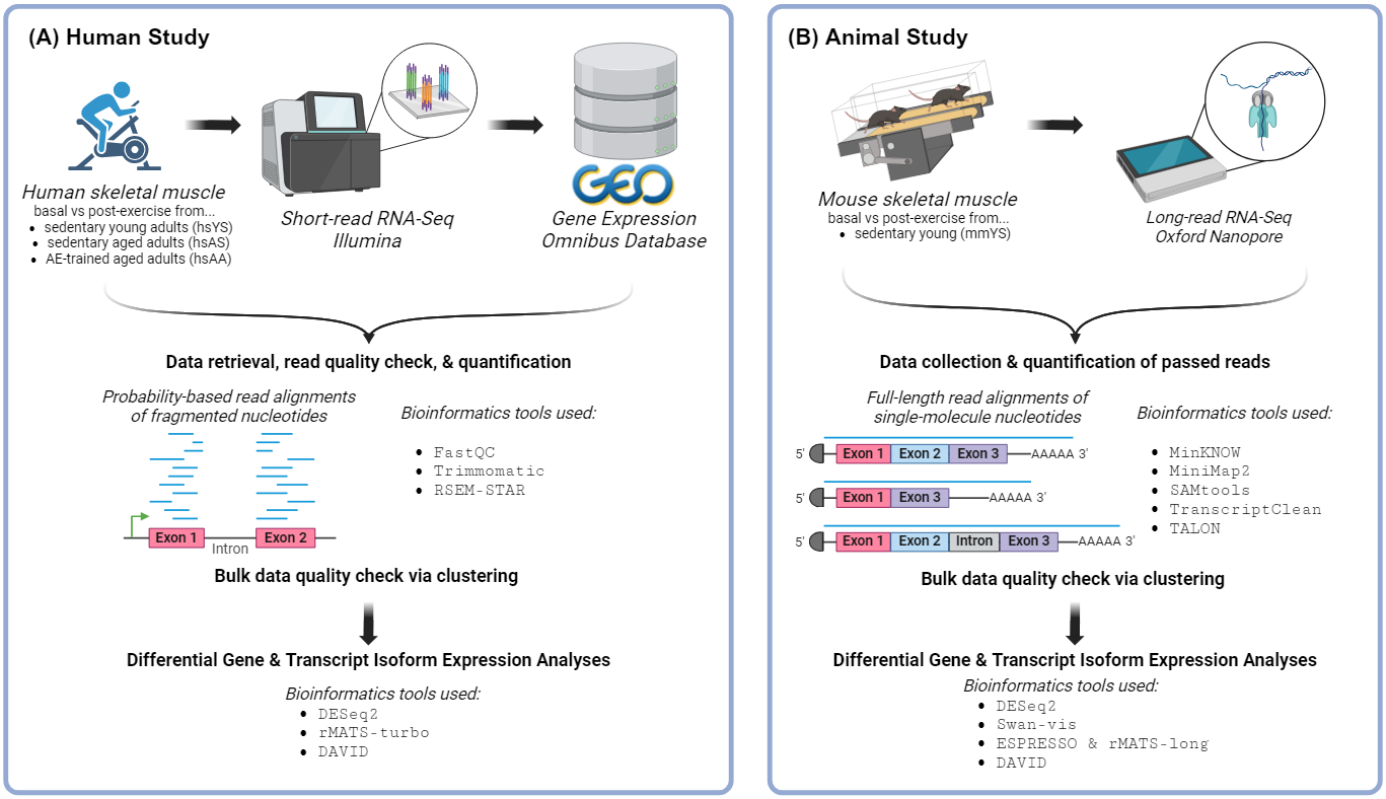
(A) Human Study
Human skeletal muscle
basal vs post-exercise from...
sedentary young adults (hsYS)
sedentary aged adults (hsAS)
AE-trained aged adults (hsAA)
Short-read RNA-Seq
Illumina
Gene Expression
Omnibus Database
Data retrieval, read quality check, & quantification
Probability-based read alignments
of fragmented nucleotides
Exon 1
Intron
Exon 2
Bioinformatics tools used:
FastQC
Trimmomatic
RSEM-STAR
Bulk data quality check via clustering
Differential Gene & Transcript Isoform Expression Analyses
Bioinformatics tools used:
DESeq2
rMATS-turbo
DAVID
(B) Animal Study
Mouse skeletal muscle
basal vs post-exercise from...
sedentary young (mmYS)
Long-read RNA-Seq
Oxford Nanopore
Data collection & quantification of passed reads
Full-length read alignments of
single-molecule nucleotides
5'
Exon 1
Exon 2
Exon 3
AAAAA 3'
Intron
Bioinformatics tools used:
MinKNOW
MiniMap2
SAMtools
TranscriptClean
TALON
Bulk data quality check via clustering
Differential Gene & Transcript Isoform Expression Analyses
Bioinformatics tools used:
DESeq2
Swan-vis
ESPRESSO & rMATS-long
DAVID

# Figure 2.

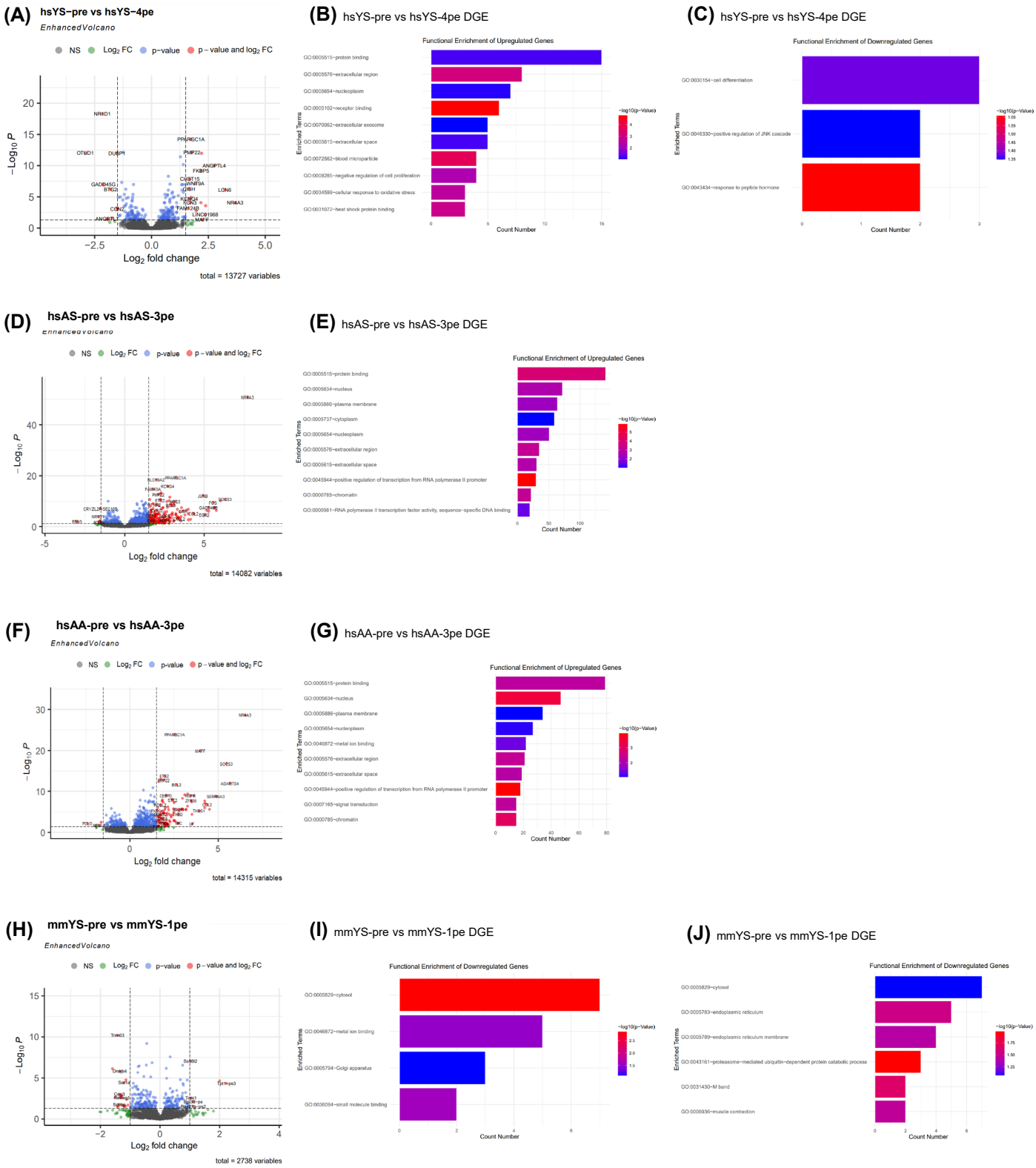
(A) hsYS−pre vs hsYS−4pe
EnhancedVolcano
NS
Log2 FC
p−value
p − value and log2 FC
−Log10 P
Log2 fold change
total = 13727 variables
(B) hsYS-pre vs hsYS-4pe DGE
Functional Enrichment of Upregulated Genes
GO:0005515−protein binding
GO:0005576−extracellular region
GO:0005654−nucleoplasm
GO:0005102−receptor binding
GO:0070062−extracellular exosome
GO:0005615−extracellular space
GO:0072562−blood microparticle
GO:0008285−negative regulation of cell proliferation
GO:0034599−cellular response to oxidative stress
GO:0031072−heat shock protein binding
Enriched Terms
Count Number
−log10(p−Value)
(C) hsYS-pre vs hsYS-4pe DGE
Functional Enrichment of Downregulated Genes
GO:0030154−cell differentiation
GO:0046330−positive regulation of JNK cascade
GO:0043434−response to peptide hormone
Enriched Terms
Count Number
−log10(p−Value)
(D) hsAS-pre vs hsAS-3pe
EnhancedVolcano
NS
Log2 FC
p-value
p − value and log2 FC
−Log10 P
Log2 fold change
total = 14082 variables
(E) hsAS-pre vs hsAS-3pe DGE
Functional Enrichment of Upregulated Genes
GO:0005515−protein binding
GO:0005634−nucleus
GO:0005886−plasma membrane
GO:0005737−cytoplasm
GO:0005654−nucleoplasm
GO:0005576−extracellular region
GO:0005615−extracellular space
GO:0045944−positive regulation of transcription from RNA polymerase II promoter
GO:0000785−chromatin
GO:0000981−RNA polymerase II transcription factor activity, sequence−specific DNA binding
Enriched Terms
Count Number
−log10(p−Value)
(F) hsAA-pre vs hsAA-3pe
EnhancedVolcano
NS
Log2 FC
p-value
p − value and log2 FC
−Log10 P
Log2 fold change
total = 14315 variables
(G) hsAA-pre vs hsAA-3pe DGE
Functional Enrichment of Upregulated Genes
GO:0005515−protein binding
GO:0005634−nucleus
GO:0005886−plasma membrane
GO:0005654−nucleoplasm
GO:0046872−metal ion binding
GO:0005576−extracellular region
GO:0005615−extracellular space
GO:0045944−positive regulation of transcription from RNA polymerase II promoter
GO:0007165−signal transduction
GO:0000785−chromatin
Enriched Terms
Count Number
−log10(p−Value)
(H) mmYS-pre vs mmYS-1pe
EnhancedVolcano
NS
Log2 FC
p-value
p − value and log2 FC
−Log10 P
Log2 fold change
total = 2738 variables
(I) mmYS-pre vs mmYS-1pe DGE
Functional Enrichment of Downregulated Genes
GO:0005829−cytosol
GO:0046872−metal ion binding
GO:0005794−Golgi apparatus
GO:0036094−small molecule binding
Enriched Terms
Count Number
−log10(p−Value)
(J) mmYS-pre vs mmYS-1pe DGE
Functional Enrichment of Downregulated Genes
GO:0005829−cytosol
GO:0005783−endoplasmic reticulum
GO:0005789−endoplasmic reticulum membrane
GO:0043161−proteasome−mediated ubiquitin−dependent protein catabolic process
GO:0031430−M band
GO:0006936−muscle contraction
Enriched Terms
Count Number
−log10(p−Value)

**Figure 3.**

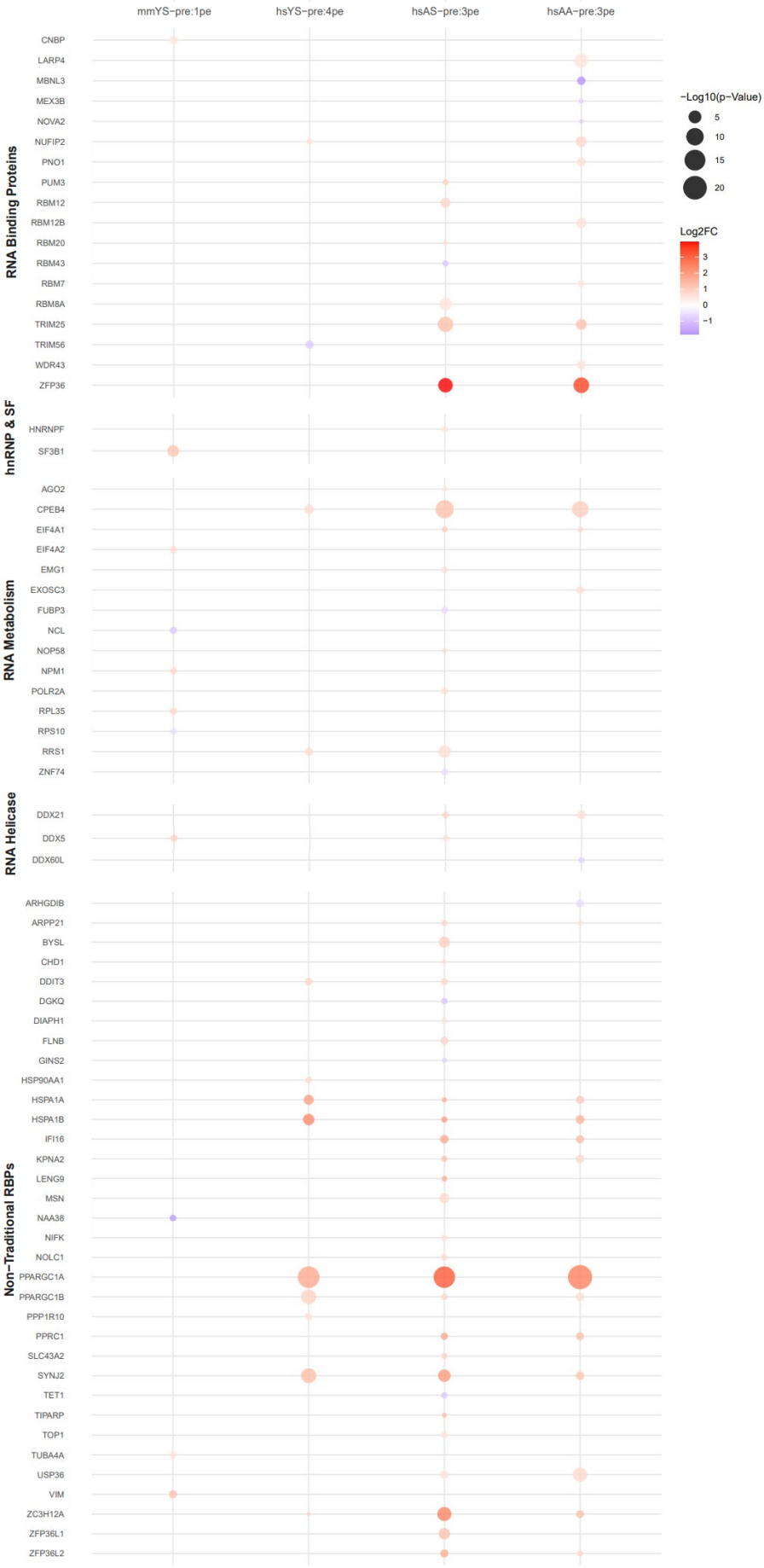
mmYS−pre:1pe
hsYS−pre:4pe
hsAS−pre:3pe
hsAA−pre:3pe
RNA Binding Proteins
CNBP
LARP4
MBNL3
MEX3B
NOVA2
NUFIP2
PNO1
PUM3
RBM12
RBM12B
RBM20
RBM43
RBM7
RBM8A
TRIM25
TRIM56
WDR43
ZFP36
hnRNP & SF
HNRNPF
SF3B1
RNA Metabolism
AGO2
CPEB4
EIF4A1
EIF4A2
EMG1
EXOSC3
FUBP3
NCL
NOP58
NPM1
POLR2A
RPL35
RPS10
RRS1
ZNF74
RNA Helicase
DDX21
DDX5
DDX60L
Non−Traditional RBPs
ARHGDIB
ARPP21
BYSL
CHD1
DDIT3
DGKQ
DIAPH1
FLNB
GINS2
HSP90AA1
HSPA1A
HSPA1B
IFI16
KPNA2
LENG9
MSN
NAA38
NIFK
NOLC1
PPARGC1A
PPARGC1B
PPP1R10
PPRC1
SLC43A2
SYNJ2
TET1
TIPARP
TOP1
TUBA4A
USP36
VIM
ZC3H12A
ZFP36L1
ZFP36L2
−Log10(p−Value)
5
10
15
20
Log2FC
3
2
1
0
−1

**Figure 4.**

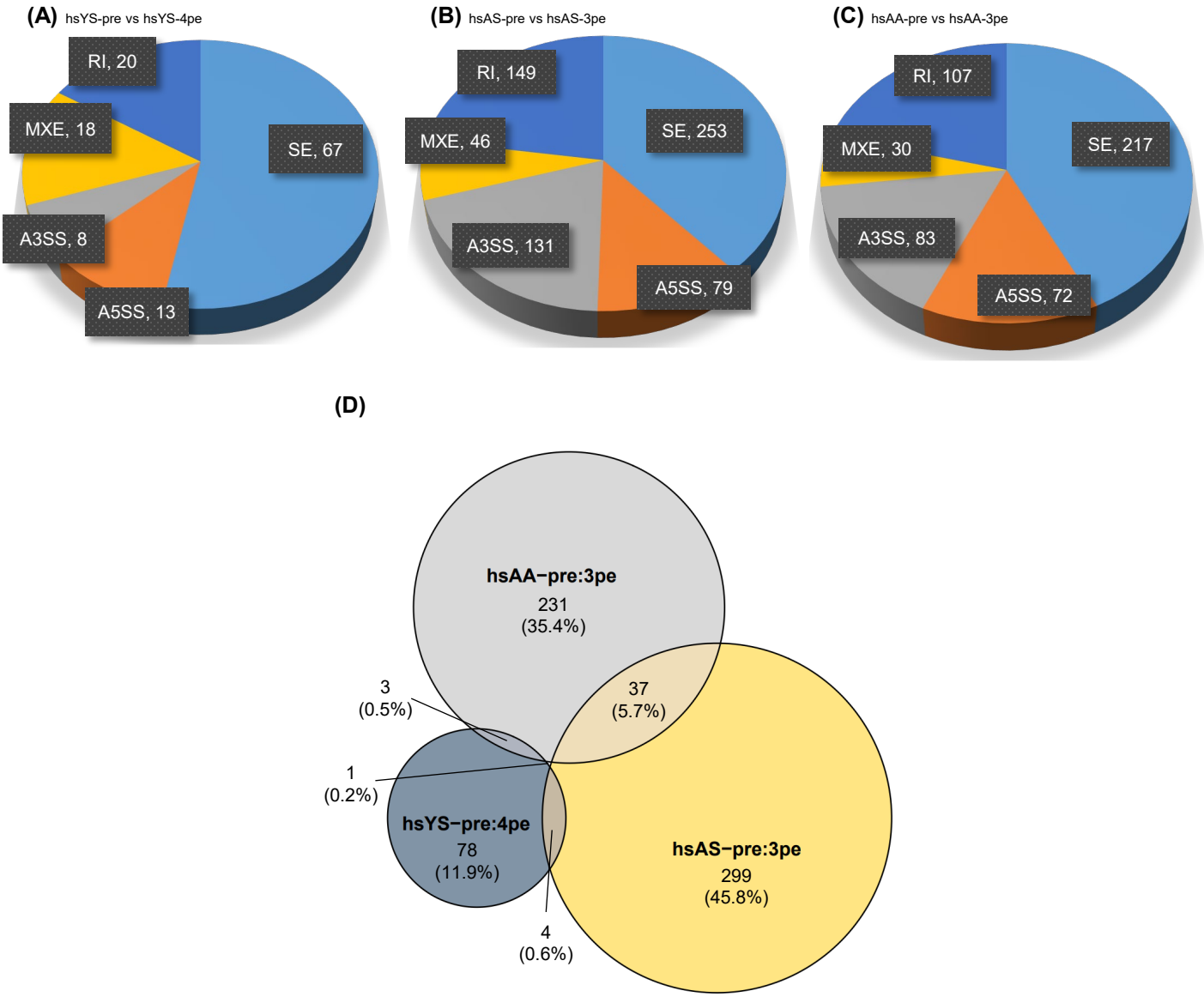
(A) hsYS-pre vs hsYS-4pe
RI, 20
MXE, 18
SE, 67
A3SS, 8
A5SS, 13
(B) hsAS-pre vs hsAS-3pe
RI, 149
MXE, 46
SE, 253
A3SS, 131
A5SS, 79
(C) hsAA-pre vs hsAA-3pe
RI, 107
MXE, 30
SE, 217
A3SS, 83
A5SS, 72
(D)
hsAA−pre:3pe
231
(35.4%)
37
(5.7%)
3
(0.5%)
1
(0.2%)
hsYS−pre:4pe
78
(11.9%)
hsAS−pre:3pe
299
(45.8%)
4
(0.6%)

**Figure 5.**

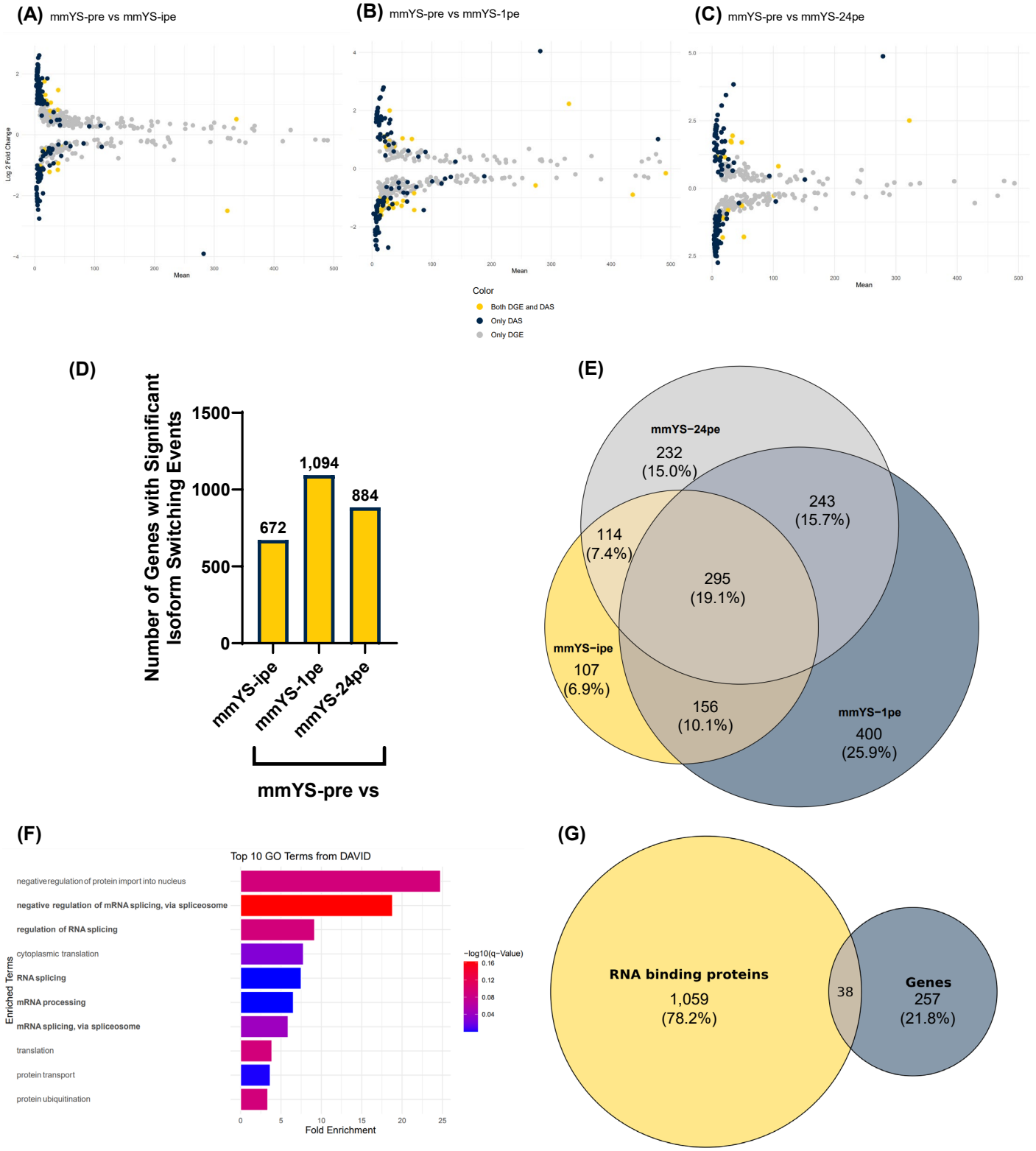
(A) mmYS-pre vs mmYS-ipe
(B) mmYS-pre vs mmYS-1pe
(C) mmYS-pre vs mmYS-24pe
Log 2 Fold Change
Mean
Color
Both DGE and DAS
Only DAS
Only DGE
(D)
Number of Genes with Significant Isoform Switching Events
1500
1000
500
0
672
1,094
884
mmYS-ipe
mmYS-1pe
mmYS-24pe
mmYS-pre vs
(E)
mmYS−24pe
232 (15.0%)
243 (15.7%)
114 (7.4%)
295 (19.1%)
mmYS−ipe
107 (6.9%)
156 (10.1%)
mmYS−1pe
400 (25.9%)
(F)
Top 10 GO Terms from DAVID
negative regulation of protein import into nucleus
negative regulation of mRNA splicing, via spliceosome
regulation of RNA splicing
cytoplasmic translation
RNA splicing
mRNA processing
mRNA splicing, via spliceosome
translation
protein transport
protein ubiquitination
Enriched Terms
Fold Enrichment
−log10(q−Value)
(G)
RNA binding proteins
1,059 (78.2%)
38
Genes
257 (21.8%)

**Figure 6.**

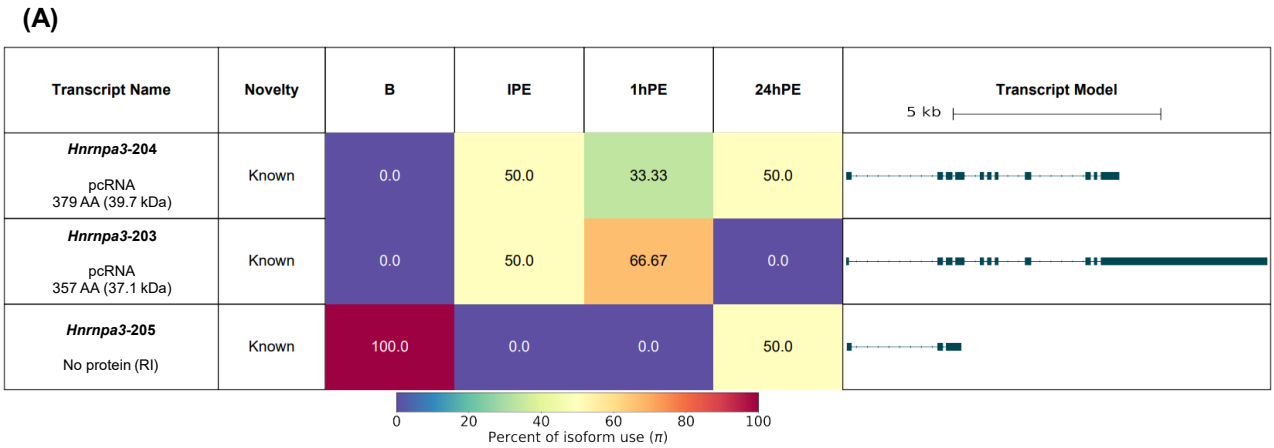
(A)
Transcript Name
Novelty
B
IPE
1hPE
24hPE
Transcript Model
5 kb
Hnrnpa3-204
pcRNA
379 AA (39.7 kDa)
Known
0.0
50.0
33.33
50.0
Hnrnpa3-203
pcRNA
357 AA (37.1 kDa)
Known
0.0
50.0
66.67
0.0
Hnrnpa3-205
No protein (RI)
Known
100.0
0.0
0.0
50.0
0
20
40
60
80
100
Percent of isoform use (π)

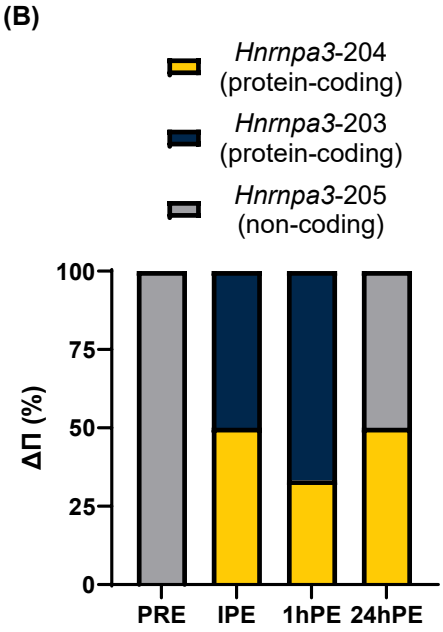
(B)
Hnrnpa3-204
(protein-coding)
Hnrnpa3-203
(protein-coding)
Hnrnpa3-205
(non-coding)
ΔΠ (%)
100
75
50
25
0
PRE
IPE
1hPE
24hPE

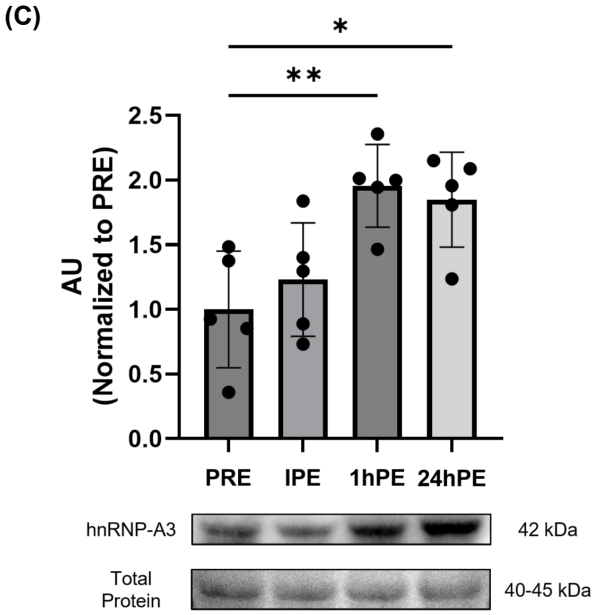
(C)
*
**
AU
(Normalized to PRE)
2.5
2.0
1.5
1.0
0.5
0.0
PRE
IPE
1hPE
24hPE
hnRNP-A3
42 kDa
Total
Protein
40-45 kDa

**Figure 7.**

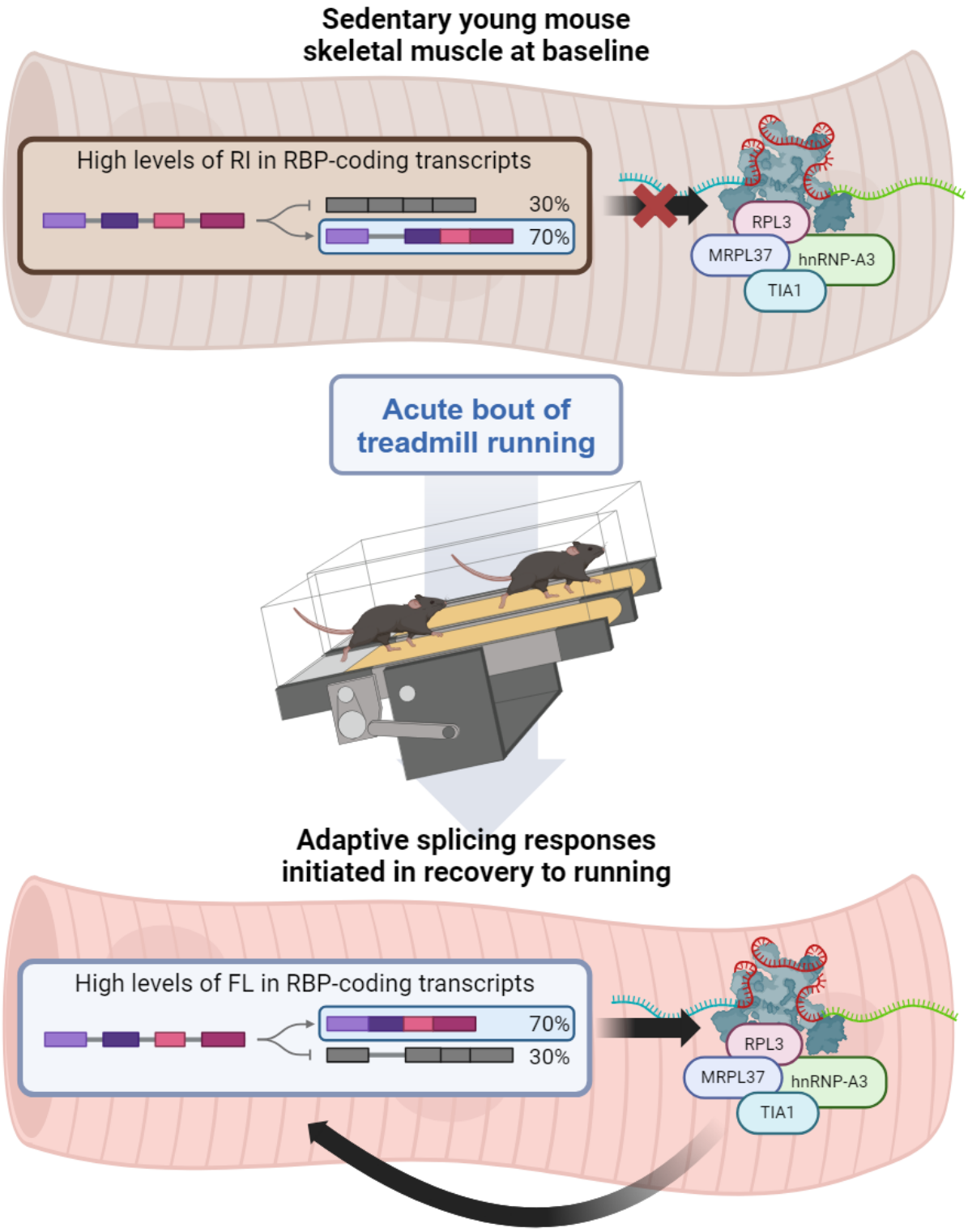
Sedentary young mouse skeletal muscle at baseline
High levels of RI in RBP-coding transcripts
30%
70%
RPL3
MRPL37
hnRNP-A3
TIA1
Acute bout of treadmill running
Adaptive splicing responses initiated in recovery to running
High levels of FL in RBP-coding transcripts
70%
30%
RPL3
MRPL37
hnRNP-A3
TIA1